A range-gated pulsed ultrasonic Doppler flowmeter

by

Gerardo Alfredo Canzonieri

A Thesis Submitted to the
Graduate Faculty in Partial Fulfillment of the
Requirements for the Degree of
MASTER OF SCIENCE

Major: Biomedical Engineering

Approved:

Signatures have been redacted for privacy

for the graduate college

Iowa State University
Ames, Iowa

1981

TABLE OF CONTENTS

INTRODUCTION

The use of low-power continuous wave ultrasound for transcutaneous detection of blood flow was first demonstrated in 1959 (1). Since then the technique has found many different clinical applications in which the Doppler shift frequencies from a continuous wave (C.W.) ultrasonic beam reflected from some moving structure are analyzed to provide a measure of the velocity of the structure. See, for example, Wells (2). In a system in which the transmitter and the receiver are stationary and the reflector is moving, we have

$$f_D = (2\ v\ f_o/c) \cos \Theta\ , \qquad (1)$$

where f_D = Doppler shift frequency, MHZ

v = velocity of reflector toward transducer, m/sec

c = ultrasonic propagation velocity, m/sec

Θ = angle of attack, degrees

f_o = carrier frequency, MHZ.

The angle of attack, Θ, is the angle between the direction of movement and the effective direction of the ultrasonic beam.

Figure 1 is a block diagram showing the arrangement of a typical Doppler frequency shift detector (3). The receiver may be considered to be a single-sideband superheterodyne with zero intermediate frequency, the leakage from the transmitter and reflections from stationary structures providing the local oscillator power. The modulation frequency is the Doppler shift frequency.

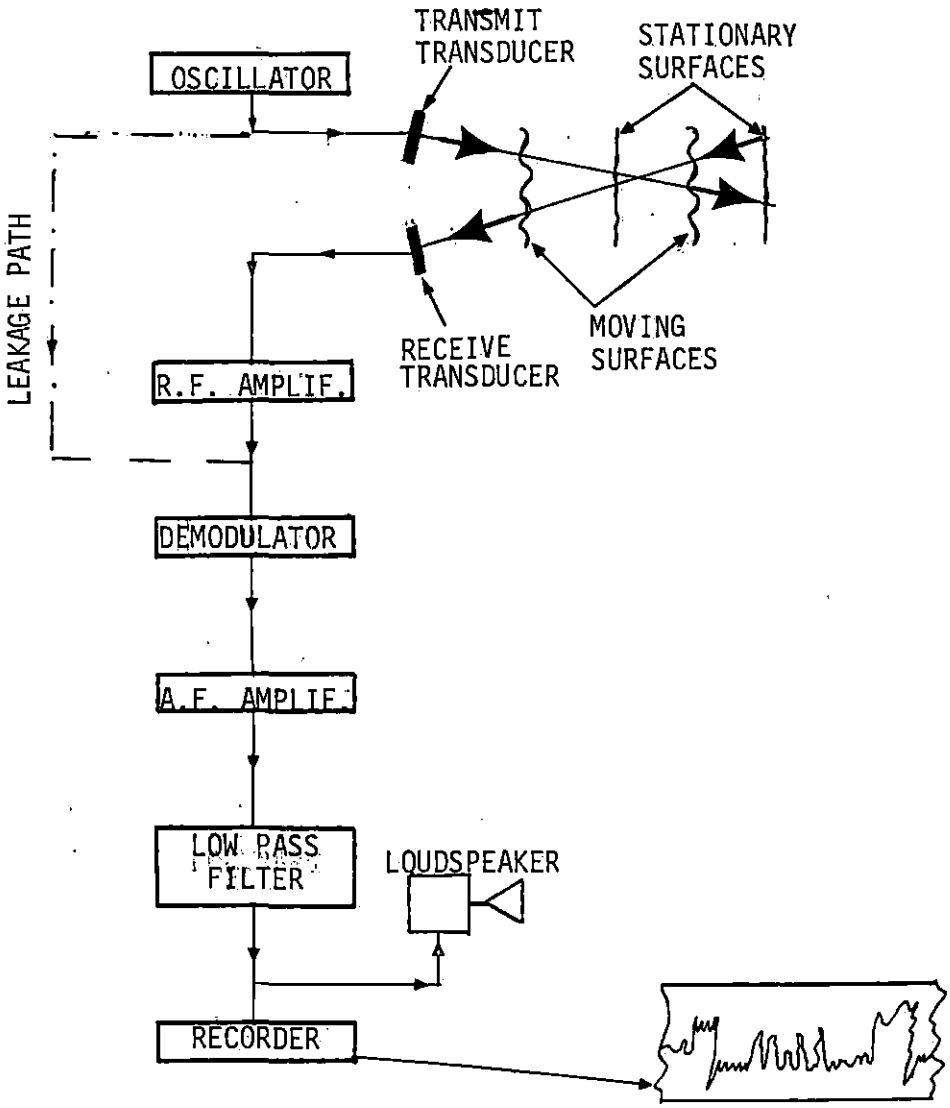

Figure 1. Typical continuous wave Doppler frequency shift system. From Wells (3)

In biological soft tissues, c is about 1500 m/sec, and the Doppler shift frequency f_D is about 1110 Hz if f_o = 8 MHz, $\Theta = 0^o$ and v = 10 cm/sec. Thus, moving structures within the body, such as cardiac valves and muscles, and flowing blood, give Doppler-shifted signals which fall in the audible range.

The output from C.W. Doppler frequency shift detectors can be interpreted by the ear or by simple frequency analysis systems. Thus, resolution is provided both in angle and frequency (3). Wells (3) considers three main clinical areas in which the Doppler method is of established value. These are in cardiology (4, 5, 6), obstetrics (7, 8, 9, 10), and the diagnosis of peripheral vascular disease (11). The principal applications and methods of analysis have been reviewed in which several moving structures lie in the ultrasonic beam (3). It is possible to use band-pass filters to separate the required Doppler information from the received audio signal. The ear is especially effective in detecting foetal and placental Doppler signals in obstetrics, particularly when such complicated sounds occur simultaneously.

The value of the Doppler frequency shift detector as a diagnostic aid would be enhanced if a method were to be devised to separate moving targets according to range. A similar technique that was applied in radar was used for ultrasound by Esmlie and McConnell (12). The system, illustrated in Figure 2, works equally well with ultrasound (3). By pulsing the acoustic emission and detecting the Doppler shift of the echo at selected depths, it is possible to determine both the velocity and the position of moving interfaces. Within certain limitations, this approach overcomes the lack of range resolution in the C.W. Doppler devices. Such instruments may permit quantification of flow by being able to measure the

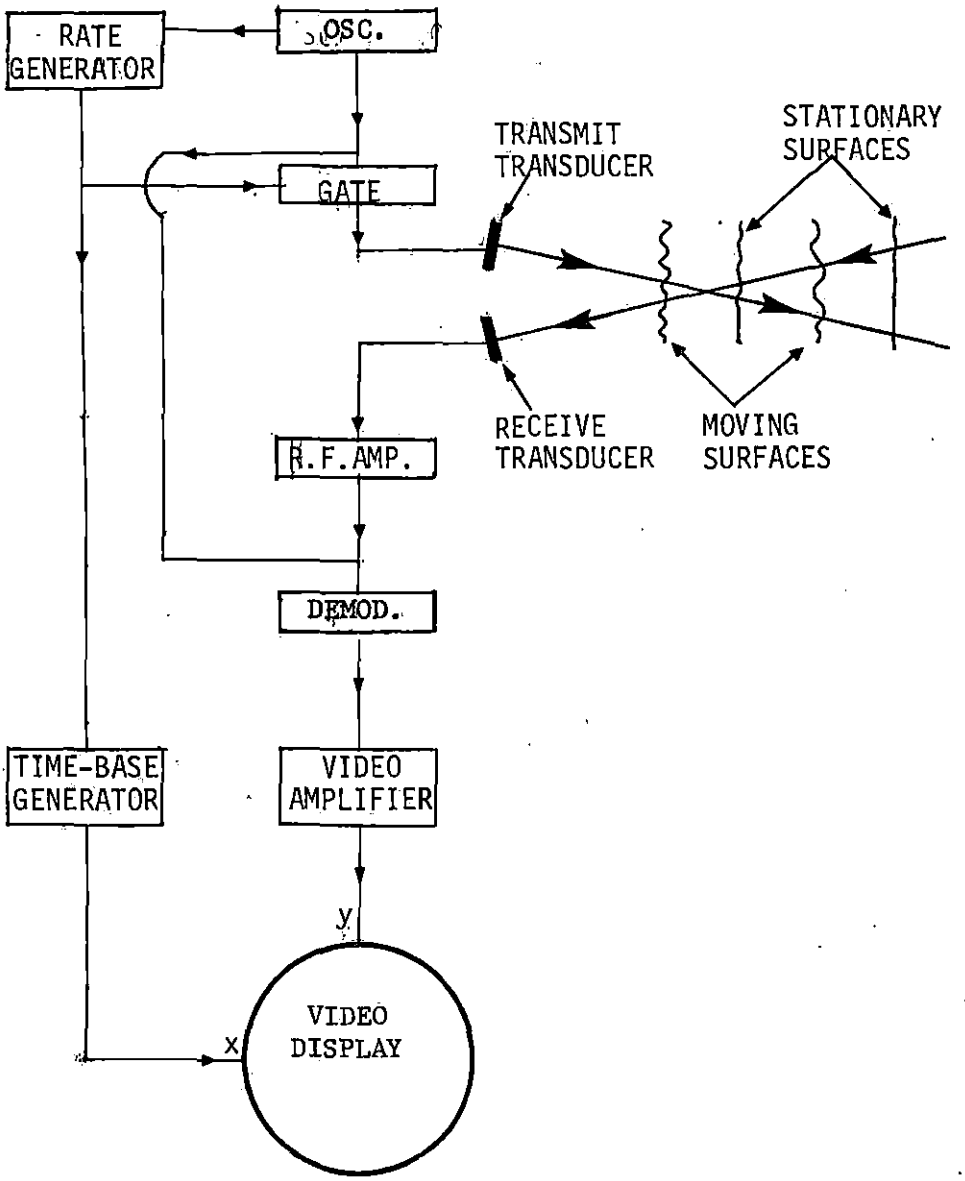

Figure 2. Block diagram of pulsed Doppler frequency shift system, that would display beat frequencies from moving structures on an A-scope display. From Wells (3)

average velocity from the velocity profile, determine the vessel diameter, and triangulate the orientation of the flow vector with respect to the beam axis (13).

Theoretical Limitations of Pulsed Doppler

The first general requirement in the design of a pulsed Doppler ultrasonic system is to achieve a satisfying S/N ratio in the return echo from the moving target. The most obvious approach is to increase the transmitter power, although this is limited by the need to keep the ultrasonic intensity within the body to an acceptable level. Fortunately, the biological response to pulsed ultrasound seems to be proportional to the average rather than the peak power level provided that the pulse length is not too long. It is possible to use quite high transmitted power in the pulse while maintaining a low average power (14).

Wells (3) suggests that a C.W. system producing an intensity of less than 40 mw/cm^2 may be used without time restriction. In a pulsed system, the power of the pulse will be higher than this value.

If a very safe level of 20 mw/cm^2 is assumed, it is easy to calculate the order of power output required from the transducer amplifier. For a transducer of 1 cm^2 area, with a transmission efficiency assumed to be 15%, operating at a duty cycle of 0.01, the pulse power will be as follows:

$$\left(\frac{.02\ W}{cm^2}\right)(1\ cm^2)\left(\frac{100}{15}\right)\left(\frac{1}{.01}\right) \cong 13\ W$$

The selection of the master oscillator frequency will influence the amplitude of the returned signal.

Since the intensity of the backscattered signal from red blood cells is proportional to (frequency)^4, while the absorption coefficient in soft tissue is approximately proportional to frequency, the optimum frequency will depend on the depth and dimensions of the target blood vessel and the nature of the overlying tissue (14). The signal-to-noise ratio (S/N) expression is given by[1]

$$\frac{S}{N} \propto \frac{f_o^4}{f_o R^2} \cdot e^{-2\alpha f_o R} \tag{3}$$

where α is the soft tissue attenuation coefficient, dB/MHZ/cm

R is the depth, cm

f_o is the center frequency, MHZ.

When this equation is differentiated with respect to frequency and the result set to zero, the optimal frequency, f_o, equals $\frac{3}{2\alpha R}$. If the attenuation γ is equal to (Np/MHZ/cm), it follows that[2]

$$f_o = \frac{15 \log e}{\gamma R} \text{ MHZ}, \tag{4}$$

and for $\gamma = 0.5$, $f_o \cong \frac{13}{R}$ MHZ.

McLeod (15), Reid and Baker (16), and Gill (17) show in Figure 3 the conclusions of their work. However, Baker et al. (13) suggests that the frequency which has optimal signal-to-noise ratio may be as high as $\frac{30}{R}$ MHZ. This latter constant, may be regarded as indicating the highest frequency, f_o,

---

[1] Only the frequency dependent terms are included.

[2] Np = Neper; 1 Np = 4.343 dB.

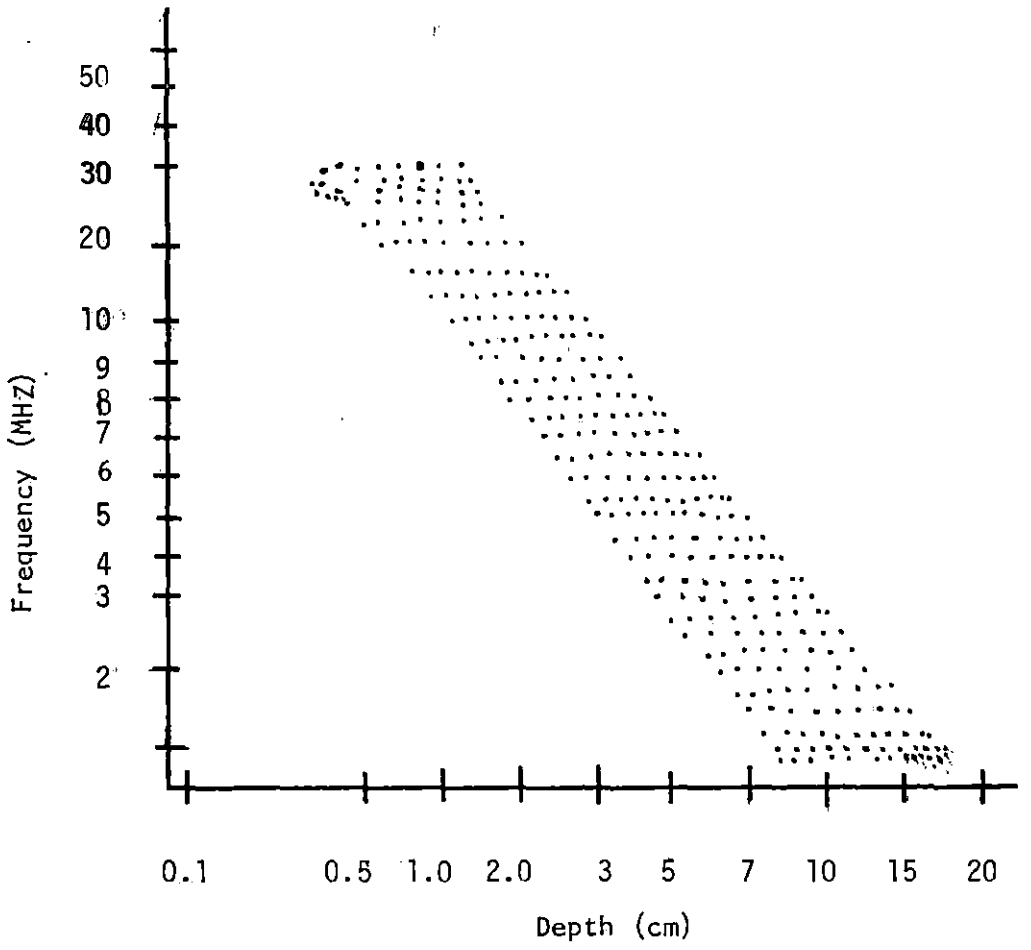

Figure 3. Calculations from several laboratories to determine the optimal frequency for maximum signal-to-noise ratio versus depth all fall within the dotted area. The precise value is influenced by a number of complex trade-offs concerning the design of specific instruments. New instrument developments will probably lead to improved signal-to-noise ratios at greater depths. From (15), (16), and (17)

that can be utilized for a given depth in centimeters which will provide an optimal signal-to-noise ratio.

Frequencies in the range 1 to 10 MHZ have been used. The higher frequencies, from 8 to 10 MHZ, offer better spatial resolution, but only over a short range of, perhaps, 30 mm. For greater penetration it is necessary to use a lower frequency, with a corresponding reduction in definition (14). Other factors which diverse the signal-to-noise ratio are related to the detailed design of the equipment, namely, the use of a low-noise receiver and a transducer with the highest possible efficiency consistent with the operating conditions.

Frequency and Range Ambiguities

In a system in which it is required to simultaneously measure range and velocity, severe constraints are imposed on the pulse repetition frequency. The highest frequency that can be analyzed without ambiguity is half the sampling frequency. This maximum frequency is the Nyqist folding frequency; above it, aliasing error occurs. For this system, the sampling frequency is equal to the pulse repetition frequency (PRF).

In fact, the maximum frequency which can be analyzed without ambiguity may be rather less than half the sampling frequency predicted by theory. Peronneau et al. (18) included a graph of indicated velocity against frequency which showed a rapid departure from the ideal case for frequencies greater than about one third of the PRF. However, this effect seems to be due to the frequency meter used to analyze the Doppler signal (14). Experimental results have shown that dynamic spectral analysis allows accurate measurement of frequency components to virtually the theoretical limits.

Because it is not possible to remove the high frequency components of the Doppler spectrum before the sampling process without degrading system performance, the PRF must be increased to insure an adequate sample rate.

If the PRF is increased, there may be insufficient time for echoes from a previously transmitted burst to have decayed below the detection threshold before the next pulse occurs. Under such circumstances it would be possible for range ambiguities to occur, i.e., the sampled signal would be a combined echo related to two successive transmitted pulses.

It is not difficult to show that the maximum unambiguous range, d (max), and the PRF are not independent. The sampling theorem gives

$$f_D < \frac{PRF}{2} . \tag{5}$$

while the time between successive pulses must be at least equal to the time for an acoustic wave packet to reach the maximum range and return.

$$\frac{1}{PRF} > \frac{2\ d}{c} \tag{6}$$

Hence, $f_D \cdot d_{max} < |c/4|$. In the clinical trials conducted to date, it has been possible to choose a compromise value of PRF, which gives an adequate sample rate without introducing range ambiguities. However, the problem may be more acute if higher velocities are to be measured (14).

Sample volume

In the case of a single transducer disc, which functions alternately as a transmitter and receiver, the receiver volume geometry is controlled

in an axial direction by the number of cycles in the transmitted pulse burst and by the transient response of the transducer.

In the near field the lateral boundary of the sensitive region is usually taken as a cylinder extending out from the transducer and having the same radius, while in the far field, the beam diverges and the energy is combined into a number of lobes. For most practical purposes the energy in the side lobes is much less than in the main lobe and can therefore be ignored. Baker et al. (13) suggests a phasor description as a very good tool in understanding the relationships between the various components of the returned signal (amplitude and modulation format) and the various types of signal detection schemes which can be used to derive the Doppler information. Before analyzing the pulsed case, it is convenient to examine the simpler case of the C.W. device. The device has separate transducers for transmitting and receiving. Projecting ultrasound into the direction of the vessel from the transmitter generates two primary components of this signal in the receiving element: the leakage phase, ϕ_L, and the Doppler shift component, ϕ_D, backscattered from the moving red blood cells as shown in Figure 4a. Both of these signals are picked up by the receiving transducer and summed together to form the receiver input, $\phi_L + \phi_D$, as shown in Figure 4b.

When these two components combine at the receiving transducer, amplitude modulation and phase modulation occur. The rate of change of the phase of the sum, with respect to a reference phase, ϕ_R, corresponds to the Doppler shift rate. The magnitude of the sum also varies at the Doppler shift frequency giving a form of amplitude modulation. The ratio of the two signals, ϕ_D/ϕ_L, determines the overall sensitivity of the

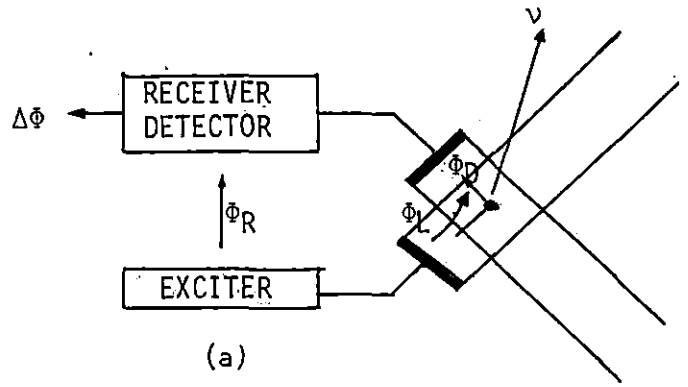

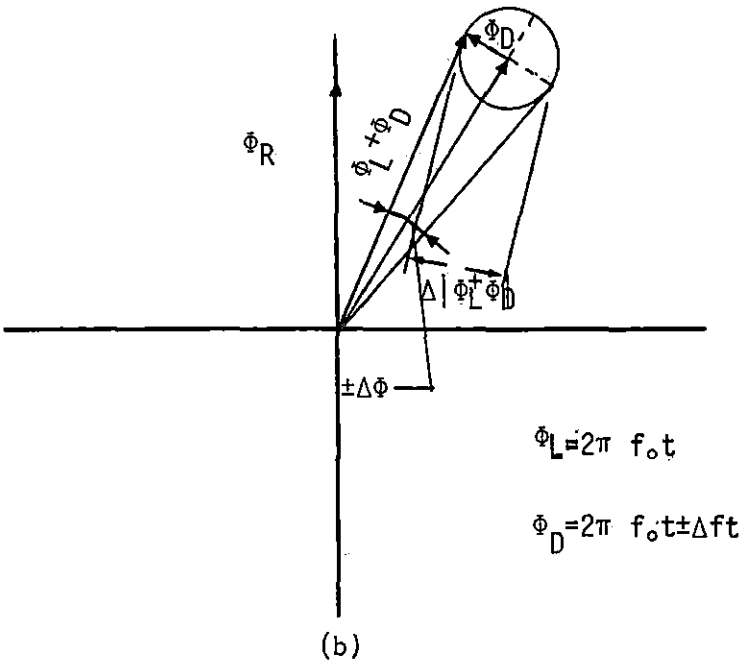

Figure 4a. The signal picked up by the receiver detector amplifier in a continuous wave Doppler consists of a Doppler shifted component, Φ_D, and a leakage component, Φ_1. The Doppler shift is derived by comparing the sum of $\Phi_D + \Phi_L$ with Φ_R, the reference signal

Figure 4b. The phase relationships between the Doppler component, Φ_L, and the reference signal, Φ_R. The sum of $\Phi_D + \Phi_L$ produces both phase and amplitude modulation

Doppler device. The larger the backscattered component, ϕ_D, is with respect to the leakage component, ϕ_L, the more sensitive the device will be, since a larger change in phase, $D\phi$, will occur. The ideal device would reduce the leakage phase, ϕ_L, to zero. In a typical Doppler device, the signal ϕ_D will be some 40 to 50 dB below ϕ_L, giving an amplitude modulation of the order of 1%. The corresponding magnitude of the phase modulation for this signal relationship gives a $\pm \Delta\phi = \pm 0.57^{o}$ at the carrier frequency, f_o. The same type of analysis can also be used to describe the return signal in a pulsed Doppler device. In contrast to the continuous wave Doppler, a pulsed Doppler has a region of flow sensitivity which is determined by the duration and delay of a receiver range gate from the transmitted burst. The pulsed device is sensitive only to velocities occurring within the sample volume.

In the example shown in Figure 5A, the signal has two components: one, ϕ_D, the Doppler signal, returning from the common volume between the sample volume and the vessel; the other, a larger component ϕ_L, is backscattered from the region within the sample volume but outside the vessel lumen. In this case, the ratio ϕ_D/ϕ_L will be small. In Figure 5B, a much larger vessel is being scanned; the sample volume is small respect to the vessel lumen and the ratio ϕ_D/ϕ_L will be much larger. These cases are summarized in Figure 5C (13). In case B, a large vessel with small sample volume, the ratio ϕ_D/ϕ_L is low when the sample is outside the vessel and then rises to a fixed value inside the vessel. The output stays at that level while the sample volume is entirely within the vessel and then falls on the far side. In case A, with the small vessel and large sample volume, the ratio is low. It reaches a lower value and returns to a low level

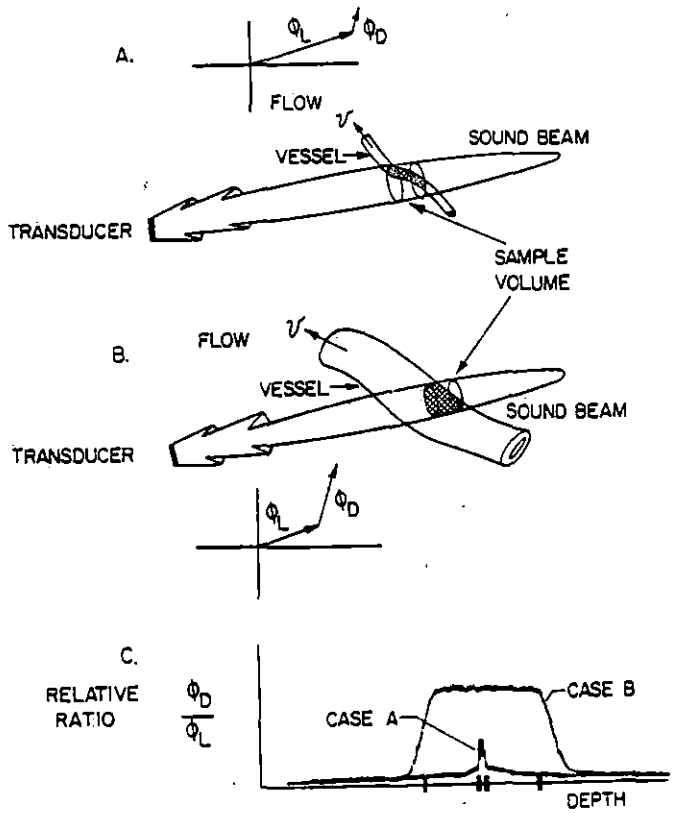

Figure 5. In a pulsed Doppler device, the region of sensitivity can be represented by a small cylinder along the axis of the sound beam, (A). The signal detected from this region will consist of two components, the leakage phase, Φ_L, and the Doppler shift phase, Φ_D. The magnitude of the Doppler component, Φ_D, will depend on the dimensions of the common volume between the vessel and the sample volume as well as the scattering characteristic of blood. This ratio will change significantly when the sample volume is small with respect to the vessel dimensions, (B). The maximum sensitivity is achieved when the sample volume is entirely within the lumen of the vessel. The relative ratio of the Doppler shift component to the leakage component determines the overall sensitivity of the pulsed Doppler device, (C). In case (B), the amplitude of the backscattered signal will reach a constant level if the sample volume is smaller than the vessel lumen. In case (A), the intensity of the backscattered signal will be smaller and never reach the same magnitude when the vessel is smaller than the sample volume. From Baker et al. (13)

beyond the vessel. The ratio will always be smaller in the case where the sample volume is equal to, or smaller than the vessel diameter. Roevros (19) also concluded that the total backscattered power is only dependent on the magnitude of the measuring volume, the particle concentration (assuming single scattering), and the power scattered per particle. The effects described here are primarily dependent on the fact that the measuring volume is changing as the sample volume moves through the vessel, except in the cases where the sample volume is smaller than the vessel, in which case the relative ratio between ϕ_D/ϕ_L becomes constant for as long as the sample volume is within the vessel (13).

Dynamic range and resolution

Within the limitations imposed by by noise and the maximum transmitted power, the maximum useful dynamic range of the echoes received in conventional medical diagnostic pulse-echo systems is about 100 dB. This dynamic range is shared between the variations in echo amplitude at fixed distances, and the attenuation of echoes which increases with distance (2).

Wells (2) defines the resolution of any imaging system in several ways. For example, the resolution may be taken to be equal to the reciprocal of the minimum distance between two point targets at which separate registration can just be distinguished on the display. An alternative definition, equivalent in concept and usually more convenient, is to specify the reciprocal of the distance which appears on the display, to be occupied by a point target on the field. In ultrasonic systems two different resolutions are of chief importance. These are the lateral (in azimuth or elevation) resolution, which describes the resolution along the

beam diameter normal to the axis, and the range resolution, which is the resolution along the axis. Both these quantities depend on a number of factors, including the distance from the transducer. The influence of distance is particularly important in the case of lateral resolution (2). Another concept which is helpful to introduce here, is that of the resolution cell. The resolution cell is the volume of material within which the interaction producing the data takes place. Except in the simplest and most idealized situation, the resolution cell may have several values of volume, a different value for each interaction; and for any particular interaction, it may have a volume which changes with time and frequency. Thus, there is not simple answer to the question, "What is the resolution of this ultrasonic system?"

The range resolution of a pulse echo system is better than its practical lateral resolution. The range resolution defines the ability of the system to separate targets spaced close together in range and is thus equal to the reciprocal of the effective duration of the pulse (2). The estimation of range resolution on the basis of pulse slope and dynamic range becomes more difficult if the pulse is propagated in media with dispersive absorption (2). The situation is more complicated, although the magnitude of the overall effect is reduced by the restricted bandwidth of the receiving system.

In practice it is necessary to compromise between a long pulse (which gives poor range resolution but is relatively free from dispersion and noise) and a short pulse (which has good range resolution but is stretched by dispersion and has a poor signal-to-noise ratio because of its large frequency bandwidth) (2). The usual remedy is to make the bandwidth

of the electronics sufficiently wide so that the transducer is the effective bandwidth-limiting component.

Baker et al. (13) describes two systems in which the Doppler signal velocity information can be reduced.

Noncoherent pulse Doppler In any biological system, the echoes returning from moving interfaces are always mixed with non-Doppler clutter signals from stationary interfaces. All these signals mix at the receiving transducer to produce an amplitude modulated signal. The frequency of the modulation corresponds to the Doppler difference signal. Such a system is sometimes said to be externally coherent. The noncoherent scheme uses a gated or pulsed transmitting signal, usually a pack of sine waves at an appropriate ultrasonic frequency. Range gating is used to select an echo for detection from a predetermined depth. The Doppler component is detected from the range gated sample by a square-law diode detector. The primary difficulty of this system is erratic fluctuations in the detected Doppler signal due to variations in the mixing ratio of the Doppler and clutter signals.

Coherent pulse Doppler The return echoes from moving interfaces are phase modulated as well as amplitude modulated. If a range gated sample of the return echo is compared with a replica of the transmitted signal in a phase detector, the Doppler components can be easily derived.

It is convenient to use amplitude limiting in the receiving amplifier to remove the amplitude variations in the echoes (13). Despite the fact that a noncoherent system is easier to build than a coherent system, the difficulty mentioned before makes the former system unattractive.

Range and Velocity Resolution

General Characteristics of Doppler Systems

In virtually all applications of ultrasonic Doppler techniques to cardiovascular measurements, one is interested not only in blood velocity (or flow rate), but also in the dimensions of the region over which the velocity estimation is made. In this sense, the overall performance of an ultrasonic Doppler velocimeter is strongly related to its simultaneous velocity and spatial resolutions. There are numerous system characteristics that influence the resolution of a given Doppler instrument. However, the fundamental parameters that determine the space/velocity resolution common to all types of Doppler instruments are the transducer sound beam and the waveform of the transmitted signal (13).

Acoustic beam effects In order to investigate the effect of the acoustic beam pattern on space/velocity resolution, consider a C.W. system transmitting a sinusoidal waveform. A particle moving with a velocity v through such a sound field is shown in Figure 6a. The signal is obtained by mixing (multiplying) the transmitted waveform with the backscattered Doppler shifted signal. As both of these signals are continuous sinusoidal waves, they are represented in the frequency domain as impulses. Multiplication in the time domain is equivalent to convolution in the frequency domain. The result is shown in Figure 6b. Note that the frequency spectrum of the Doppler signal, after filtering off the higher frequency component, consists of a single impulse at Δf, a frequency directly related to the particle velocity v, by the equation

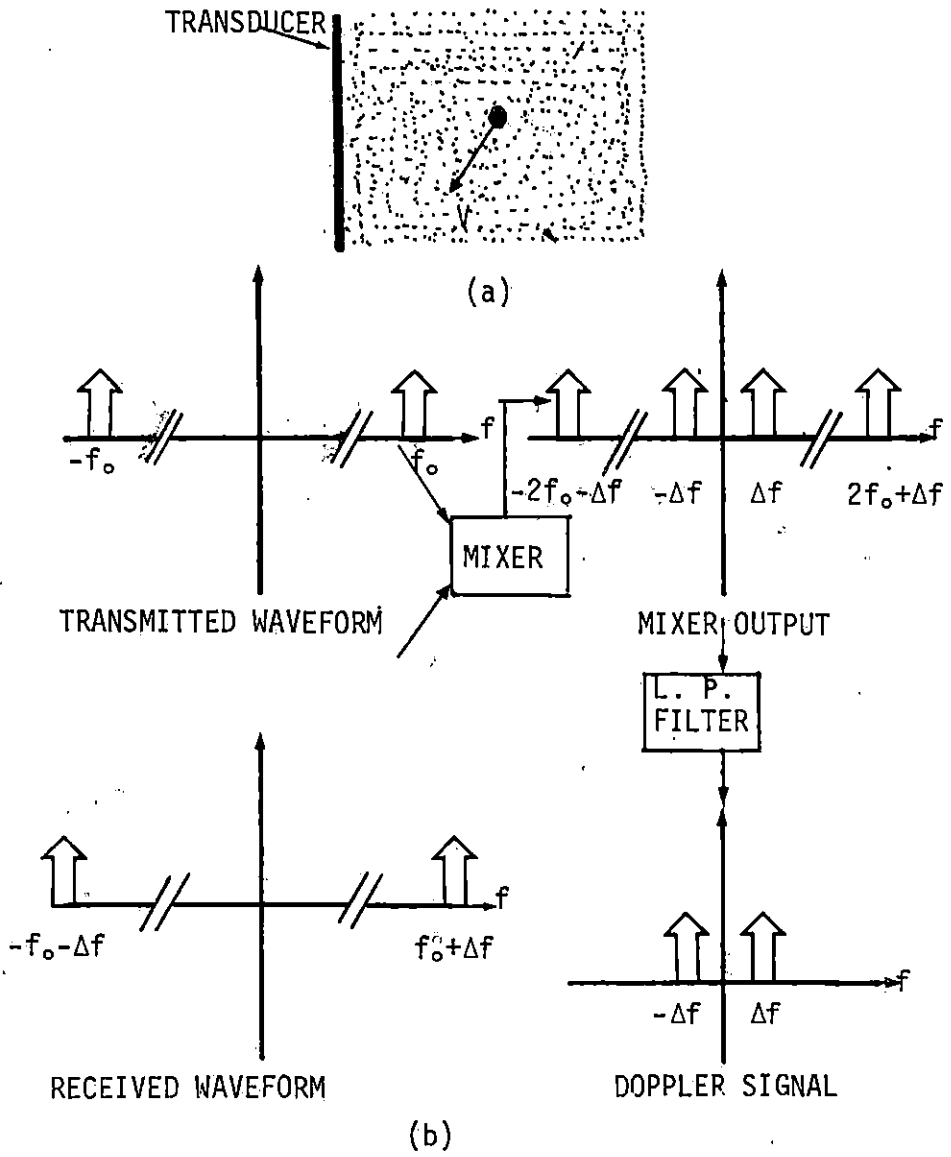

Figure 6. C.W. Doppler system with an acoustic sound field of infinite extent showing the acoustic sound field (a) and the frequency domain representation of the signal processing (b). From Baker et al. (13)

$$\Delta f = \frac{2f_o}{c} |v \cos \theta| \qquad (7)$$

where the terms are as defined in equation 1. Since the Doppler spectrum is an impulse in this case, the measurement of $v \cos \theta$ is unambiguous. The case is a perfect representation of velocity resolution and is related to the fact that the particles backscatter sound energy for an infinite length of time (13).

Consider a more realistic case in which the particle moves through a finite width acoustic beam as shown in Figure 7a. The particle backscatters acoustic energy only for the length of time it is in the sound beam. Thus, the returning signal is a finite sinusoidal waveform. In the frequency domain, such a signal is ideally represented as a $(\frac{\sin x}{x})^2$ function (13). The Doppler signal resulting from the mixing and filtering process described above is shown in Figure 7b. The resulting Doppler spectrum has a frequency spread which is inversely proportional to the time the particle spends in the sound beam. The spread can be considered an ambiguity in the velocity measurement, since the ability to resolve two different velocities degrades with the width of the frequency spectrum. Brody (20) obtained these same results for the case of a large number of randomly distributed scatterers in the sound beam. Baker et al. (13) has shown in several experiments that velocity resolution is related to the time available for measurements. There is also a trade-off between spatial and velocity resolution. Decreasing the beam width improves the lateral resolution of the system at the expense of velocity resolution. This trade-off is

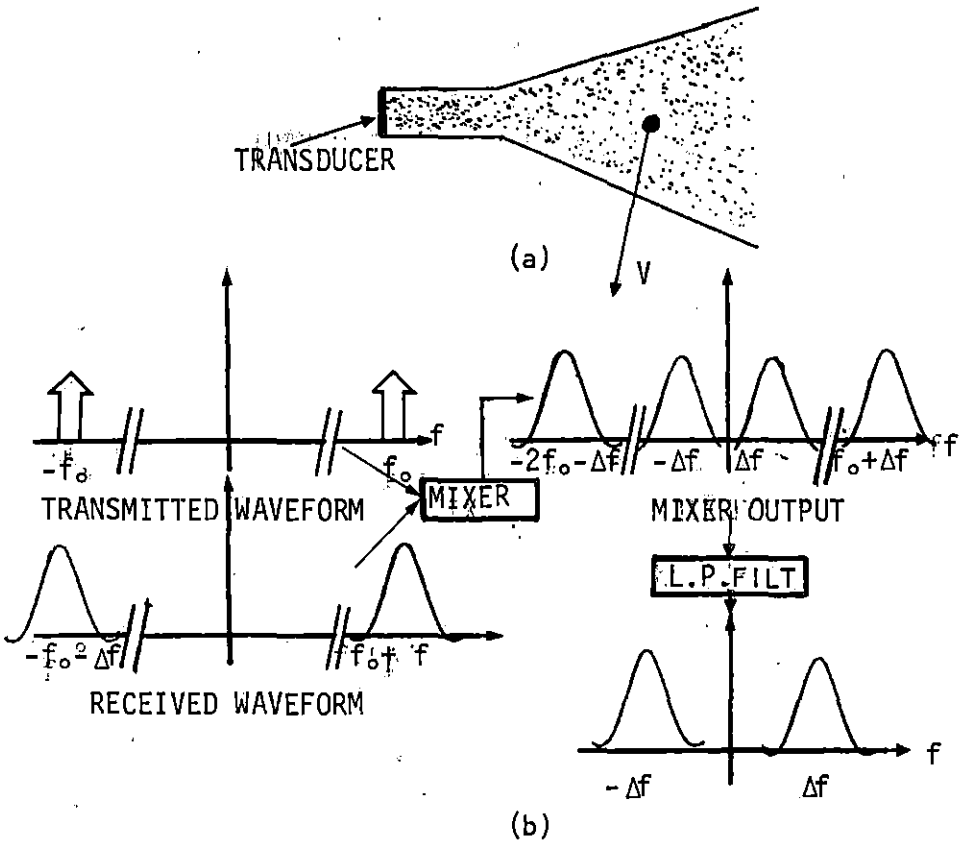

Figure 7. C.W. Doppler system with an acoustic sound field of finite extent showing the acoustic sound field (a) and the frequency domain representation of the signal processing, (b). From Baker et al. (13)

evident in numerous aspects of Doppler instrumentation. Although not a direct result of the uncertainty relation of quantum mechanics,

$$\Delta f \cdot \Delta t \gtrsim 1. \tag{8}$$

This expression simply states that to obtain a good spatial resolution the signal must be concentrated in the time domain, while for good velocity resolution the signal must be concentrated in the frequency domain. Fourier transform theory, however, tells us that these conditions cannot be met simultaneously. The discussion above was developed for C.W. Doppler velocimeters (13).

Transmitted signal effects Baker et al. (13), in his development of the theory, considered that the spatial resolution was completely determined by the sound field. The bandwidth of the signals used was zero. However, it is known from radar theory that good range resolution can also be achieved by transmitting a waveform of nonzero bandwidth.

Baker et al. (13) has shown that velocity resolution is directly related to temporal length of the returning signal. One might conclude that for simultaneous range and velocity resolution the time-bandwidth (T.B.) product should be maximized. However, numerous other factors also influence resolution. The problem is too complex to be completely described by the T.B. product (13). Rihaczek (21) has also shown that the upper band for a measure of error in simultaneous range and velocity estimation is directly proportional to the T.B. product. Thus, a large T.B. product does not guarantee accuracy.

Due to the importance of the transmitted waveform with respect to simultaneous range/velocity resolution, a large number of possibilities have been investigated in radar applications and some of these have also been used for ulstrasonic applications in medicine (13).

Baker et al. (13) noted, however, that there is no "perfect" waveform. The optimum waveform depends on the characteristics of the target and the environment in which the target is located. Baker discussed briefly the general characteristics of a number of different transmitted waveforms that have been implemented or proposed for medical ultrasonic Doppler systems.

Pulsed phase coherent signal In the phase coherent pulsed system, a constant frequency carrier is amplitude modulated to obtain short harmonic bursts which are phase coherent from pulse to pulse (22). The backscattered signal is demodulated and sampled at time τ from the transmission of the last burst. The sampled signal then corresponds to backscattered energy originating at distances equal to

$$\frac{c}{2}\left(\tau + \sum_{n=1}^{\infty} \frac{n}{f_r}\right) \tag{9}$$

where f_r is the pulse repetition rate.

Normally, one relies on the fact that no targets are located at the ambiguous ranges represented by the summation term in the above equation, or that attenuation of the transmitted signal is sufficient to rule out the possibility of detectable signals coming from the ambiguous region. There are similar discrete velocity ambiguities associated with the fact that

the pulse repetition interval is regular. However, one normally picks the pulse repetition frequency at least twice the highest expected Doppler frequency to satisfy the Nyquist sampling theorem. In this way, the complete spectrum of the Doppler signal will be contained in the frequency range,

$$0 \leq f \leq f_r/2. \tag{10}$$

The lower bound for the pulse repetition frequency given above unfortunately leads to the major disadvantage of the pulsed phase coherent system. For the signal to return from the desired region before the next burst is transmitted, the maximum range is limited to

$$R_{max} = \frac{c}{2} \frac{1}{f_r} . \tag{11}$$

Otherwise, at the time signals returned from the desired range, signals from ranges nearer the transducer could also arrive. A limitation of the pulsed phase coherent Doppler system is caused by the fact that the duration of the transmitted burst must be kept short to maintain fine range resolution. This requirements imposes very high ratios of peak-to-average transmitted power. Since the echo from a target to range R gives a range delay of

$$\tau = 2R/c \tag{12}$$

it can be seen by differentiation that the range resolution ΔR for a transmitted burst of duration τ_e is, at best

$$\Delta R = c\, \tau_e/2. \tag{13}$$

The ratio of peak-to-average transmitted power can be written as

$$P_p/P_a = \tau_p/\tau_e \qquad (14)$$

where τ_p is the period of the transmitted signal, equal to the inverse of the PRF. Using equations 11 and 13, this gives

$$P_p/P_a = R_{max}/\Delta R \qquad (15)$$

which is equal to at least 10^2 in any high resolution coherent system.

Specific characteristics of pulsed coherent systems

Spatial resolution In a pulsed phase coherent system, short bursts of acoustic energy are transmitted by an amplitude-modulated carrier. The returning signal is sampled at a specific delay time following the transmission of each pulse. The sampled portions of the returning signal correspond to backscattered acoustic energy originating from a specific region of space called the sample volume, whose range from the transducer is determined by the delay time (13).

The spatial resolution of a Doppler system is determined by the size of the sample volume. For a transducer of 1 cm diameter and 3 cm focal length, in a 5 MHZ system, the sample volume is typically 1 mm diameter by 2 mm long; this sample volume contains approximately 1×10^7 red blood cells, each contributing to the scattered signal. In blood flow, it is normally assumed that the blood cells represent a random distribution of scatterers (13).

The effective intensity distribution within the sample volume can be determined from the form of the transmitted signal envelope and other

system parameters. Figure 8a shows the signal applied to the transducer and the signal received from a stationary reflector. The envelope of the signal is determined by the exponential rise as the transducer is excited and the exponential decay in amplitude as the crystal oscillates. Normally the transmitter and receiver have bandwidths equal to or greater than that of the transducer. Figure 8b shows the actual transducer response.

The length of the sample volume corresponds to the distance sound travels in one half the transmitted burst duration, Δt_b, (13) or

$$\text{sample volume length} = \frac{c}{2} \Delta t_b . \qquad (16)$$

The length of the sample volume is also related to the method of sampling the returning signal. There is an additional contribution to the length equal to $\frac{c}{2} \Delta t_g$, where Δt_g is the effective observation gate time (13). In an ideal case, the sampling time equals 0; for a practical sample-hold circuit, t is $\underline{\sim}$ 0. A problem occurs at the vessel wall when the sample volume extends beyond the vessel, thus erroneously indicating flow outside the boundary (23).

As a general rule, where the geometry may not be favorable, it is desirable that the sample volume does not have a long "tail", which would make it difficult to eliminate strong interfering signals such as those caused by vessel wall motion (14).

Velocity resolution Velocity resolution is closely related to the width of the Doppler spectrum. The broader the spectrum, the more difficult

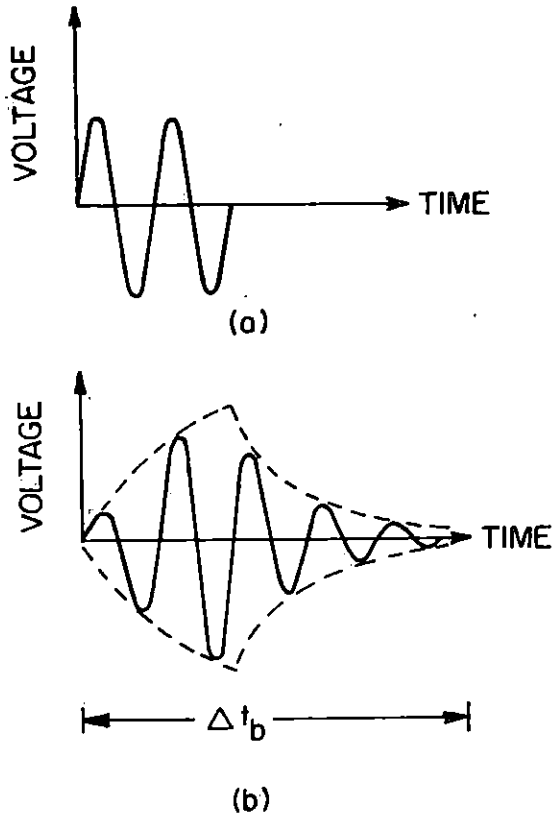

Figure 8. The transmitted signal applied to the transducer (a) and the transducer response (b). From Baker et al. (13)

it would be to measure a small shift of the spectrum (change in velocity). Factors affecting Doppler spectral broadening can be classified into instrument effects and flow-related effects (13). It is important to note that improvement in velocity resolution (narrower Doppler spectrum) leads to degradation in spatial resolution.

Spectral broadening due to flow effects Two main causes contribute to spectral broadening due to the flow effect. These can be referred to as spatial and temporal effects. Spatial effects are simply due to the fact that if velocity gradients exist in the flow field, a range of velocities of the particles moving through the sample volume will exist. This range of velocities, Δv, will result in additional frequency components in the Doppler spectrum. It is important to note that Δv is not a function of the velocity gradient alone, but is also a function of the sample volume size. Thus, gradient broadening can be reduced by reducing the sample volume size (13).

Temporal effects refer to the fact that over a given period of time the velocities of the particles moving through the sample volume may change. If the Doppler signal was viewed on a spectrum analyzer whose integration time was so long as to exceed the period of the heart cycle, the Doppler spectrum would contain the entire range of Doppler shifts present throughout the flow cycle. In other words, the time necessary to obtain a spectral estimate is small compared to the period of the heart cycle. Work by Forster et al. (24) has demonstrated that a quantitative measure of the intensity of turbulence can be made based on spectral broadening of the Doppler signal. One practical application of this phenomenon is the measurement of turbulent flow ultrasonically.

Computation of Volume Flow

The problem of quantitation

The process of making a blood velocity measurement with an ultrasonic device is indeed complex and subject to a number of errors. There are two categories of errors. One is inherent to the system or technique being utilized (systematic errors). The second arises from experimental difficulties in applying the technique (experimental errors). The choice of any technique must be made so as to minimize the effect of systematic errors on the sought after variable. Then, the technique must be implemented so as to minimize the effect of experimental errors (13).

The term "quantification", as applied to Doppler blood velocity sensing, generally refers to the accurate measurement of volume blood flow through a vessel, in units such as cc/sec.

Blood velocity measurement Ultrasonic Doppler devices for measuring blood flow should be termed velocimeters, since this is the actual parameter measured. The relation between the Doppler shift, Δf, and, the energy scattered from red blood cells and their velocity, v, is described by the already mentioned equation

$$v = \frac{\Delta f \; c}{2 \; f_o \cos \theta} \tag{17}$$

The simple equation given above masks the complexity of a Doppler measurement. It describes the situation where only one moving particle backscatters the sound field. In actual blood flow measurements, there are many

cells which are distributed over a range of velocities and space, passing in and out of the sound beam. Under these actual conditions, the Doppler shift, Δf, is not a single frequency but is a distributed quantity. This condition may limit, in certain cases, the accuracy of the velocity measurement.

Measurement of Δf The measurement of Δf is perhaps the most difficult component of Doppler velocity measurements. In any real measurement, the detected Doppler shift frequencies form a frequency spectrum. It is desired to extract the mean or first moment frequency of this spectrum since this frequency is the best approximation to the spatial average of blood velocity over the measurement region (13).

Instrument effects Instrument effects on the Doppler shift spectrum can be best dealt with if the requirements are first defined, including the maximum range and spatial extent of the measurement region and the required velocity resolution. Next, the instrument parameter which are capable of modification should be optimized for the particular measurement requirements.

The next step is perhaps the most crucial. It is the determination of the measurement region, which must be experimentally obtained. This can be accomplished using a thin jet of scatterers in a water tank to provide a line target which can be moved through the measurement region, or a moving sheet of scatterers which provides a step velocity function.

After achieving the spatial resolution requirements, the step that follows is to successfully extract meaningful information from the Doppler shift spectrum. The usual method is to employ zero-crossing detection, primarily because of the simplicity and ease of implementation of the technique. The method is simply an averaging of a train of impulses produced when the signal crosses a zero voltage threshold. However, the circuit cannot work ideally. The signal-to-noise ratio must be 30 dB or more. If not, the device cannot discriminate between the low level noise and the Doppler signal. The zero-crossing detector (ZCD) produces the root-mean-square of the frequency spectrum. Because of this type of processing, a change in flow profile will affect the output of the ZCD (25). For narrow band signals, as normally encountered when dealing with small sample regions in laminar flow, the error introduced by taking the zero crossing output as an estimate of Δf is small. For broadband signals, however, the error can amount to as much as 15% (20). The best analytical technique for dealing with the Doppler spectrum employs computer techniques. The analysis uses an adaptation of a Fast Fourier transform algorithm (FFT) but the technique is complex (26).

Transcutaneous blood flow measurements

The measurement of volume blood flow in a rigorous manner involves solving a classical equation common to engineering. The equation is as follows with modification for a Doppler device (16):

$$Q = \overline{V} A \cos \Theta \tag{18}$$

where Q = volume flow rate, cm^3/sec

$\overline{V}$ = average flow velocity over area of vessel lumen, cm/sec

A = cross sectional area of vessel lumen, cm^2

Θ = angle between sound beam axis and flow velocity vector, degrees.

The flow velocity may be determined by one of two ways. The first might be a velocity profile measurement taken across the lumen from which the average velocity can be calculated. The second approach involves using a pulsed Doppler instrument having a range gate or sample volume whose length is equal to the slant diameter of the vessel and is positioned to give the instantaneous average volume-flow (22). The two most important and difficult parameters to measure are the vessel diameter and the angle between the velocity vector and sound-beam axis (22).

Vessel distance measurement Several methods for determining the vessel diameter are possible. Each has its difficulties. The principal difficulty is related to the resolving power of the pulse Doppler range gate. At the present time, diameter is determined by noting when flow signals appear and disappear as the range gate is scanned across the lumen. Taking the difference in range at each of these points will give the diameter. The true diameter can then be computed if the angle between the transducer and the vessel is known. This method works very well on plastic tubes in a model if the beam angle is 80 degrees or more and the flow rates are high. Errors as small as 2-3 percent have been achieved. As the angle decreases, it becomes increasingly difficult to determine the exact position of the far wall. The size and shape of the sample volume appears to be the primary difficulty. The finite size of the sample volume causes the apparent vessel diameter to be larger than it actually is.

Studies to date suggest that it may be feasible to employ a correction factor to reduce resolution error. Higher ultrasonic frequencies and shorter acoustic bursts should allow the use of a smaller sample volume to reduce the error. Of course, the errors will be proportionately less as the vessel diameter increases for a given sample volume. At the present time, it may be possible to reduce diameter errors to approximately 10 percent or less if the transducer beam axis is aligned nearly normal to the vessel. This is an awkward angle since the detected Doppler shift approaches zero as the beam approaches a normal angle. If diameter is measured in this way it will be necessary to sense velocity at the same point, and at an angle that will allow suitable Doppler shifts to be accurately detected. Investigations to date suggest that an angle from 45 to 65 degrees with respect to the vessel will permit the highest easily attainable accuracy for sensing velocity (22).

Determining the blood vessel angle Transcutaneous volume-blood-flow measurements require that the angle between the vessel and sound beam be determined accurately. It would be ideal from the point of view of accurate velocity measurement if θ, the angle of attack, was zero or almost zero. Unfortunately, most of the superficial readily accessible vessels, such as the limb arteries and carotids, run more or less parallel with the surface of the body. Hence, θ is normally about 30 to 90 degrees, where the rate of change of cosine θ with respect to θ is rather rapid. There are two obvious ways of eliminating these inaccuracies. The first is to devise a system in which the

velocity measurements are independent of the angle Θ and the second is to devise some way of measuring Θ.

Three beam angle independent systems have been described in the literature (27). Unfortunately, spectral analysis is necessary if accurate values of velocity are required. The first two systems do not allow for its use. However, a cross beam system (25) using a three-part transducer (two transmitters and one receiver or one transmitter and two receivers) has been developed which incorporates an on-line spectrum analyzer. It is possible in that system to make absolute center-stream velocity measurements in the superficial vessels. The results are, to the first order, independent of the angle between the transducer and the direction of flow (28).

One way of ascertaining the value of the angle Θ is to visualize the vessel together with some set reference plane, e.g., the overlying skin. The calculation of Θ is then simply a case of combining the inclination of the probe and vessel to the reference plane (28).

The development of the equations necessary for the computation of volume-blood-flow follows. From equation 1 we have that

$$\overline{V} = (\overline{f}_D \, c)/[(2 \cos \Theta) \, (f_o)]. \tag{19}$$

Combining equation 18 with equation 19 gives

$$Q = \frac{A \, c \, \overline{f}_D}{2 \, f_o \cos \Theta} \tag{20}$$

where $\overline{f}_o$ = the average Doppler shift from profile or from full vessel sample gate, MHZ.

Since

$$A = \pi R_t^2 \tag{21}$$

where R_t = true radius of vessel, cm

and

$$R_t = R_s \sin \theta \tag{22}$$

where R_s = slant radius of vessel, cm, then

$$A = R_s^2 \sin \theta. \tag{23}$$

Substituting equation 18 into equation 21 and simplifying gives

$$Q = \frac{c \pi R_s^2 \tan \theta \sin \theta f_D}{2 f_o}. \tag{24}$$

This last equation will be used for the computation of fluid flow.

DESIGN CONSIDERATIONS

A pulsed ultrasonic Doppler flow detector of the coherent type has been built and evaluated. The system designed was based originally on a concept developed by Franklin et al. (29). A complete block diagram of the system designed as a result of this research project is shown in Figure 9.

Electronic Design

Oscillator

The selection of the oscillator frequency is dependent on several factors. Experience in the development of the C.W. Doppler has shown that 8 MHz is a good compromise frequency for detecting blood flow vessels 2-4 cm in depth. Units have been built with carriers as low as 2.25 MHz and as high as 10 MHz. It has been shown before that the optimal distance for this frequency is a trade off between transmission attentuation losses versus backscatter signal intensity. Figure 3 shows that 8 MHz is the optimal frequency for a depth of 2-4 cm in tissue. The sensitivity of the receiver will also influence the choice of transmitted frequency. Doppler echo signals can be detected at a different depth than the optimal frequency. Franklin's design included a voltage controlled oscillator (VCO) swept by a triangular wave. This made it possible to obtain flow direction when used with a product detector. For reasons that will be explained later, a VCO was not used in the work described in this thesis. Instead, a fixed frequency circuit was employed. The oscillator circuit is a tuned-drain FET oscillator in which a resonant circuit is used to determine the frequency. The output from the oscillator is a 3 volt $_{p-p}$ sinusoidal wave. A buffer circuit employing an enhancement mode N channel

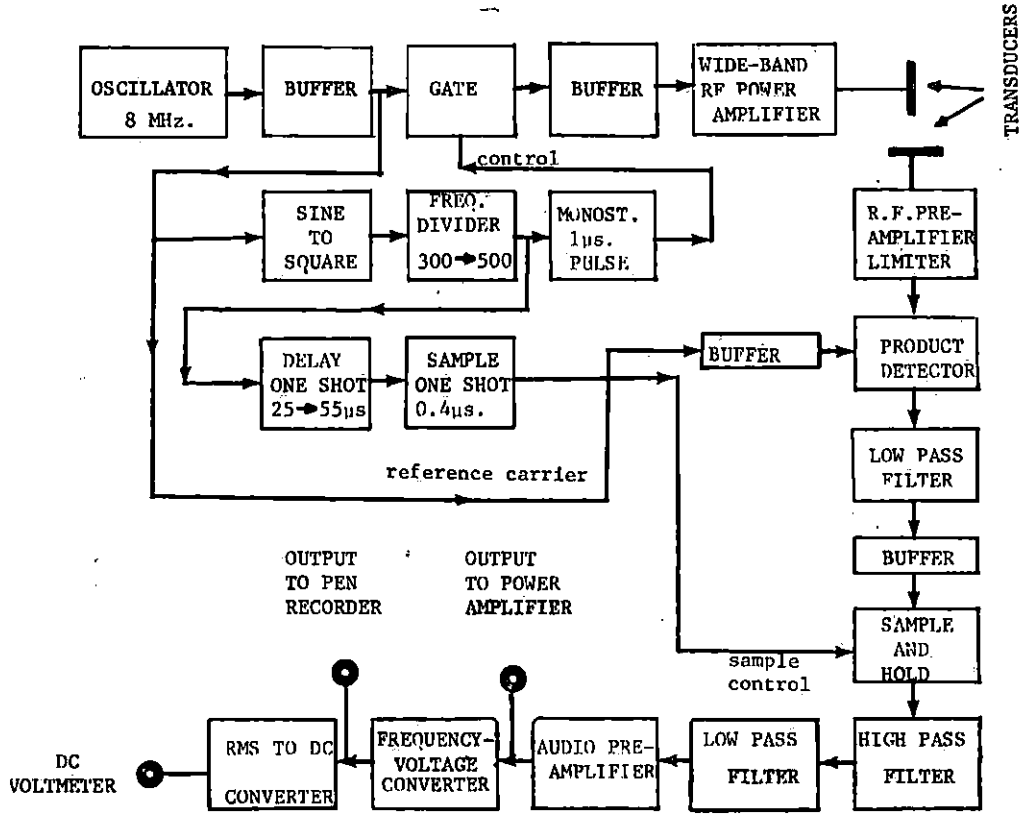

Figure 9. Complete block diagram of pulsed ultrasonic system

MOS-FET in a common drain configuration was used. This configuration was chosen in order to avoid phase shift and voltage gain. A 2.8 v_{p-p} sinusoidal wave is obtained from the output of this last stage. The oscillator and buffer circuit diagram are shown in Figure 10.

Sine-to-square converter

In order to effectively interface with standard TTL circuits, it is necessary to convert the sinusoidal wave to a square wave. The easiest way is to use a voltage comparator with clamped output. Because of the high frequency used the voltage comparator has to be fast. The choice was a National Semiconductor LM 160 which gives satisfactory response up to 10 MHZ. The connections to the integrated voltage comparator are shown in Figure 11.

Ripple counter

As was mentioned earlier, in a coherent pulsed Doppler it is essential that each transmitted acoustic burst have an identical relationship to the master oscillator. This is accomplished by dividing the oscillator frequency down to the PRF with digital integrated circuits. The in-phase output from the sine-to-square converter is divided by two-decade counters connected in series, to obtain a divide by 100 counter. This signal is followed by three digital integrated circuits connected in parallel which divide by 3, 4, or 5. A three-pole switch selects the frequency divisor. Figure 11 shows the connections of the frequency divider circuit.

The frequencies that can be selected are 26.6, 20, or 16 KHZ with an oscillator frequency of 8 MHZ. The selection of the PRF is dependent on the expected Doppler shift, depth of vessel and attenuation characteristic.

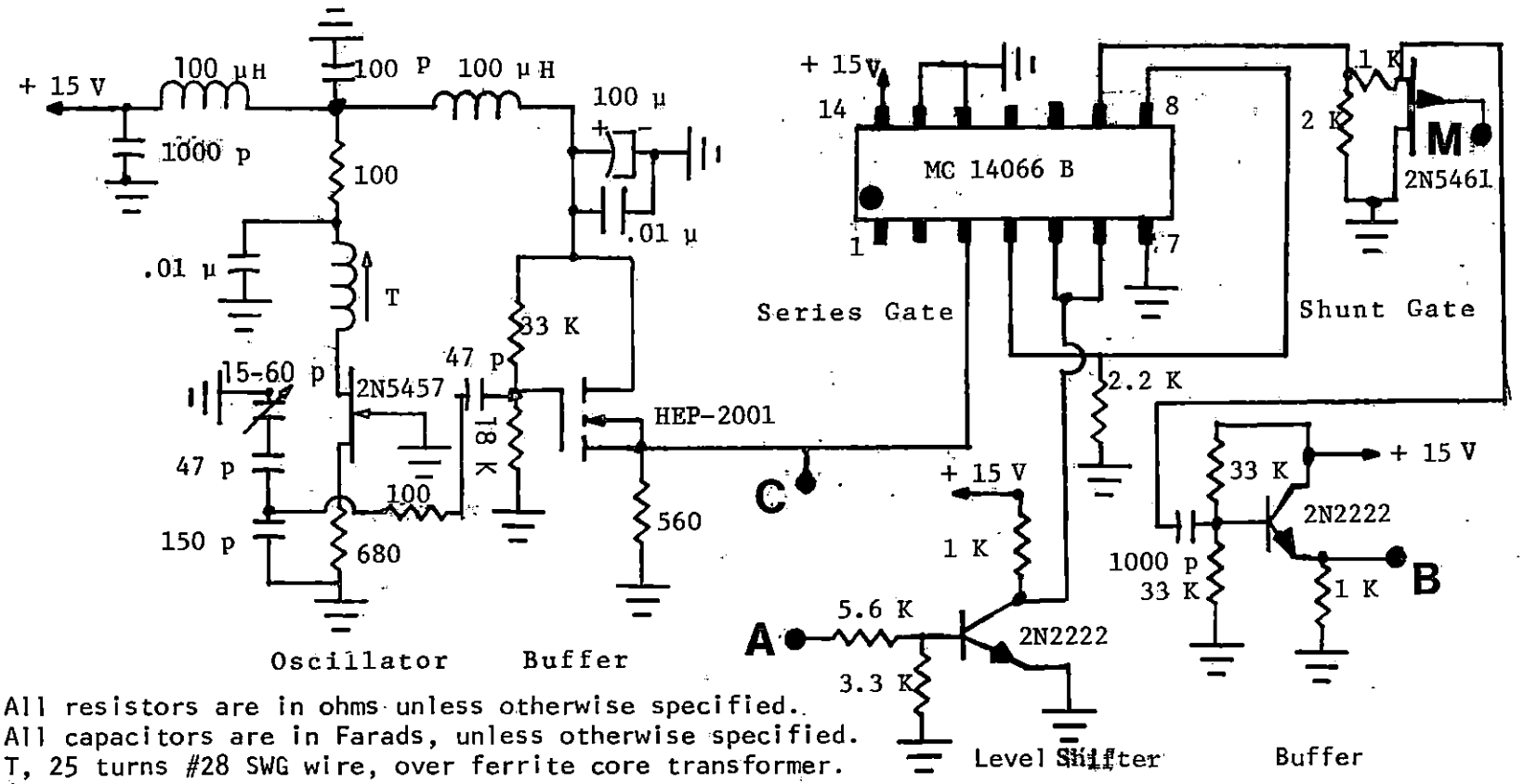

All resistors are in ohms unless otherwise specified.
All capacitors are in Farads, unless otherwise specified.
T, 25 turns #28 SWG wire, over ferrite core transformer.

Figure 10. Schematic diagram of oscillator, buffer, and gating circuits (transmitting section)

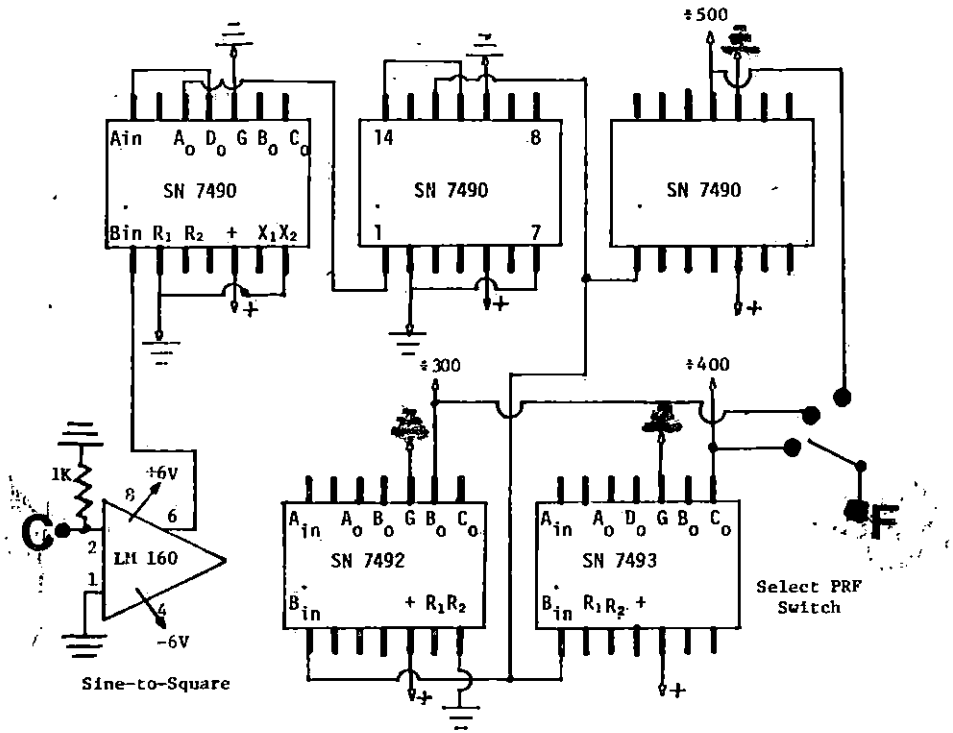

Resistor value is in Ohm. All + terminals are connected to 5 Volts positive supply.

Figure 11. Schematic diagram of sine-to-square converter and ripple counting circuits

of the tissue. In an unambiguous system, when depth and velocity are to be measured simultaneously, severe restraints are imposed. The PRF in the pulsed Doppler instrument is limited by the laws of sampling theory. If functioning in an unambigous mode, the PRF must be twice the expected Doppler difference frequency. However, when Doppler difference frequencies are high, range ambiguities can occur. This happens when echoes from the previous transmitted burst have not decayed below the detection threshold and thereby persist into the next transmission interval, making it difficult to identify which echo belongs to which transmitted burst. Also, there is insufficient knowledge about transducer losses, tissue losses and backscattered signal level to predict rigorously what PRF may be used for a given depth of measurement.

The tissue loss factors that have been investigated to date fall in the range of 1-3 dB/cm/MHZ. No reliable data are available to predict the acoustic return from a particular volume of moving blood in an ultrasonic field.

Baker et al. (13) gives a list of PRF and range depths. The combination most commonly used is given below.

PRF	Approximate depth range	Maximum Δf detectable
25 KHz	3 cm	12.5 KHz
18 KHz	4.3 cm	9 KHz

Since this system is optimized for depths of 2-4 cm (taking into account absorption losses and scattering return), the PRF used must be within 18 to 27 KHz.

Linear transmission gate and shunt gate

The PRF pulse triggers a 1 μsec one shot multivibrator which generates the gating signal for the linear transmission gate. When the gate opens, approximately 8 cycles of the master oscillator pass through to a linear power amplifier. Interposed is a shunt gate to cancel some of the feedthrough that occurs at such a high frequency. The linear transmission gate employed is a Motorola MC14066B quad analog switch. Each one of the four switches has an ON/OFF ratio of better than 50 dB at a frequency of 8 MHz. Two switches in series were used to improve this ratio. The lowest ON resistance of the switch is obtained with a supply voltage of 15 volts. A single control signal is required per switch. For normal operation, the control signal turns the switch ON when $V_{control}$ is equal to the positive supply voltage of the gate. Switch OFF occurs when $V_{control}$ is equal to V_{ss}, or ground. The output of the monostable goes from a low of 0.4 volts to a high of 3.5 volts, indicating incompatibility to control the gate. A level shifter is needed. This is performed by a transistor stage connected in a common emitter configuration. The collector pull-up resistor is connected to a 15 volt supply. Following this stage is a shunt gate using a P-channel FET (Motorola 2N 5460) that is connected as a variable resistor. This device has a gate-source voltage characteristic very well-suited to interface directly with the monostable output. Following the gate stage is an emitter follower buffer. The circuit diagram is shown in Figure 10.

Linear power amplifier

The amplitude of the reflected signal from moving blood or any other target will depend on the power applied to the transducer. This applied pulse power normally ranges between 10-30 watts and should be as large as possible while remaining within permissible dose limits.

The design specification is for a power amplifier capable of delivering between 10-30 watts into loads varying over a frequency bandwidth of 8 MHZ. Transient response is an important factor. Of course, another consideration is cost. In general, the problem of driving reactive loads in the MHZ range with a feedback amplifier is difficult.

The present research uses an amplifier previously designed and tested by Thompson (14). The design makes use of R.F. techniques, but with inexpensive "audio" transistors and easily constructed broadband transformers. The complete diagram is shown in Figure 12. The amplifier output stage uses a pair of transistors, Q_5 and Q_6, operating in push-pull with zero bias. The crossover distortion is of no consequence at typical operating output voltage levels. The push-pull transformer T_9 and balun T_{10} combine the outputs of Q_5 and Q_6 and give a single-ended output. The impedance seen by each transistor is equal to one quarter of the actual load impedance with this transformer configuration. T_5, T_6, T_7, and T_8 are all 4:1 impedance transformers and are used to match the base input impedance of Q_5 and Q_6 to the preceding stage. The driver stage uses another paid of transistors, Q_3 and Q_4, operating in push-pull and biased class AB. As with the output stage, the collector supply is fed via the push-pull transformer T_4. This method avoids problems with transient response frequently associated with R.F. chokes. Out-of-phase

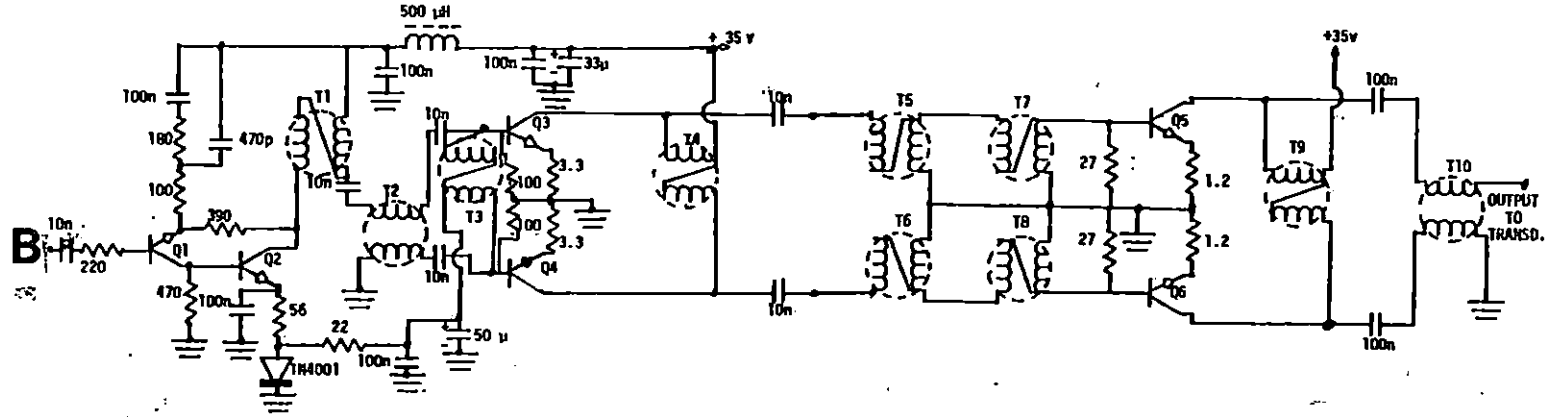

All resistors are in Ohms unless otherwise specified. All capacitors are in Farads unless otherwise specified. Q_1 MPS-U57 (Motorola)

Q_2-Q_6 2N5321 (RCA)

T_1-T_{10} 22 SWG twisted pair, 7 turns on 20 mm OD ferrite core.

Figure 12. Circuit diagram of RF wideband power amplifier

signals to the bases of Q_3 and Q_4 are provided by T_2 and T_3, while T_1 is another 4:1 impedance transformer. The transitors used are designated for audio range, with a f_t of 60 MHz, and a typical β of 100. At this frequency it is expected that the gain drops as the frequency increases. For this reason, the preamplifier Q_1 and Q_2 uses a simple frequency compensation circuit. The amplifier has a frequency response from 1 MHz to 9 MHz. This frequency response was measured with a 47 Ω load resistor connected at the output of the RF amplifier.

Transducers

The transducer used is of lithium titanate zirconate ceramic material without acoustic lenses. It has a Q of about 10. Some authors recommend the use of feedback around the power amplifier to provide dynamic damping to reduce transducer ringing. However, Thompson (14) found it difficult to use this type of configuration for his amplifier.

A typical transducer is shown in Figure 13. A diagram of the construction of this transducer is shown in Figure 14 (18). Ideally the carrier frequency leakage to the receiver input should be down at least 100 dB from the transmitted burst within few μsec after excitation. Pulse ultrasonic Doppler systems do not intrinsically avoid the transmitter-receiver leakage problem as one might think. Even if the transducer has no case echoes and if the electrical leakage from the master oscillator was reduced to a minimum, there would still exist a situation analogous to leakage in the C.W. case. The concept of spatial leakage is introduced to describe a signal-to-noise ratio difficulty characteristic to the transcutaneous application of this system. A transducer element with an

Figure 13. Close up of transmitting and receiving elements in a pulse Doppler transducer with lens. From Baker (22)

Figure 14. Cross section showing typical construction of pulse Doppler transducer. From Baker (22)

Figure 15. Comparison at regions of sensitivity for C.W. and pulsed Doppler methods. From Baker (22)

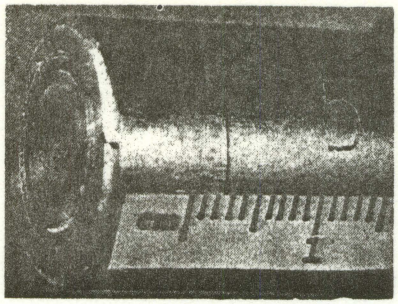

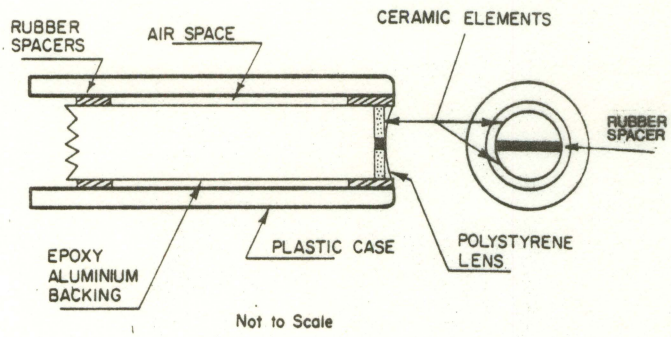
RUBBER SPACERS
AIR SPACE
CERAMIC ELEMENTS
RUBBER SPACER
EPOXY ALUMINIUM BACKING
PLASTIC CASE
POLYSTYRENE LENS
Not to Scale

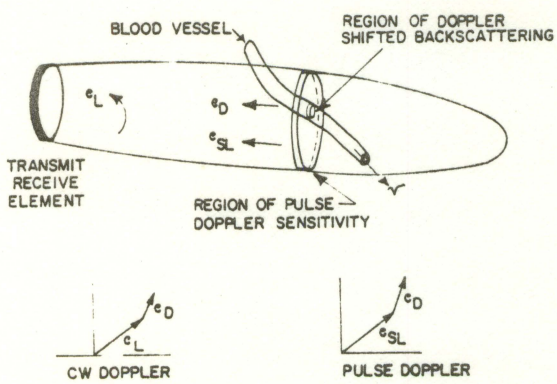
BLOOD VESSEL
REGION OF DOPPLER SHIFTED BACKSCATTERING
e_L
e_D
e_{SL}
TRANSMIT RECEIVE ELEMENT
REGION OF PULSE DOPPLER SENSITIVITY
e_D
e_L
CW DOPPLER
e_D
e_{SL}
PULSE DOPPLER

idealized beam is shown in Figure 15. The location of the disk depends on the receiver range gate delay and its thickness depends on the range dimension of the receiver resolution cell. Doppler signals will be detected from moving scatterers in the region or volume common to both the disk and the blood vessel. The region in the disk outside the vessel that has little or no motion will return an echo. This signal is called the spatial leakage and combines with the Doppler signal at the time the echo is received from the sample region (resolution cell). This sample window is sometimes called the Doppler window. The combination of spatial leakage and Doppler echoes is shown in the phasor diagram of Figure 15. Thus, ultrasonic pulse Doppler do not overcome the leakage problem simply because they are operated in a pulse mode.

Limiter and receiver

The backscattered Doppler shifted signal from the blood vessel may range in intensity from 50 dB to more than 120 dB less than the transmitted pulse amplitute. Several factors contribute to the overall losses. Baker (22) reports the components of the loses.

(1) Transmitting trasducer losses: 10-20 dB

(2) Transmitting path tissue losses: 2 dB/cm/MHz

(3) Scattering losses in blood: 20-40 dB

(4) Receiving path tissue losses: 2 dB/cm/MHz

(5) Receiving transducer losses: 10-20 dB.

For an operating frequency of approximately 8 MHZ and a vessel depth of 3 cm, the total losses are about 120-160 dB below transmitter output.

These values are approximate. No systematic study has been carried out to define the limits of these factors precisely.

Two types of receivers have been constructed and tested. The first one used a combination of MOS-FET and bipolar linear integrated circuits. The first stage used a dual gate R.F. MOS-FET device. The reason for using a dual gate device is to provide for AGC control. One microsecond before the transmitted pulse is sent out, the gain of the FET stage is reduced 60 dB. Gain reduction was necessary to prevent overload to the following stage with the single transmit-receive transducer originally used. A hard limiter stage, with Germanium diodes, was used to clamp the input voltage to about 0.5 V_{p-p}. The stage that follows was a Motorola 1590G high frequency amplifier. This device features AGC capability, although it was not used. The AGC control was set at a constant voltage. Both stages of the receiver were tuned. The overall gain of the amplifier was about 52 dB with a bandwidth of 0.8 MHz. The output also used clamping Germanium diodes in order to not overload the product detector input. This receiver performed reasonably but often oscillated. The integrated circuit had a gain-bandwidth product in excess of 220 MHz, making stability difficult to obtain.

The currently used receiver circuit is shown in Figure 16. The receiver pre-amplifier was designed using a RCA CA3022A high frequency differential amplifier. This integrated circuit features a cascode type of differential amplifier with internal diode limiter. Full limiting occurs with input voltages greater than 300 μV RMS. The output is clamped at 0.3 V_{p-p}. Two similar devices were connected in

cascade to achieve a voltage gain of 60 dB. The circuits use an RLC feedback element to achieve both D.C. and A.C. stability. The bandwidth of the cascade connection is 3 MHZ at 8 MHZ center frequency. Overload and recovery time problems were avoided by using a separate receiving transducer which also eliminated the need for diode decoupling networks between transmitter and receiver.

Product detector

The technique used in this work was a heterodyne type of detection and known as synchronous detection. In this type of detection, the incoming signal is multiplied by a reference signal generated by a local oscillator (which ideally has the same frequency and phase of the transmitted signal). The multiplied output has two components. One is a high frequency component containing a double frequency of the carrier frequency. The other output is the difference signal (carrier minus the received signal). This type of detection has the advantage that only the signals that are correlated with the transmitted pulse will be detected. Only the received signal that is amplitude-modulated and not frequency-modulated will be in the output of this type of detector. The integrated circuit used was a Motorola MC1496 single-sideband product detector. See Figure 16. This device is extremely flexible. It can be used with a myriad of power supplies. It has variable gain and a wide dynamic range that can be tailored (by a simple change of a resistor) to a specific task. The detection is accomplished with a high level carrier, used as a reference signal. The equation for the gain with this carrier level is

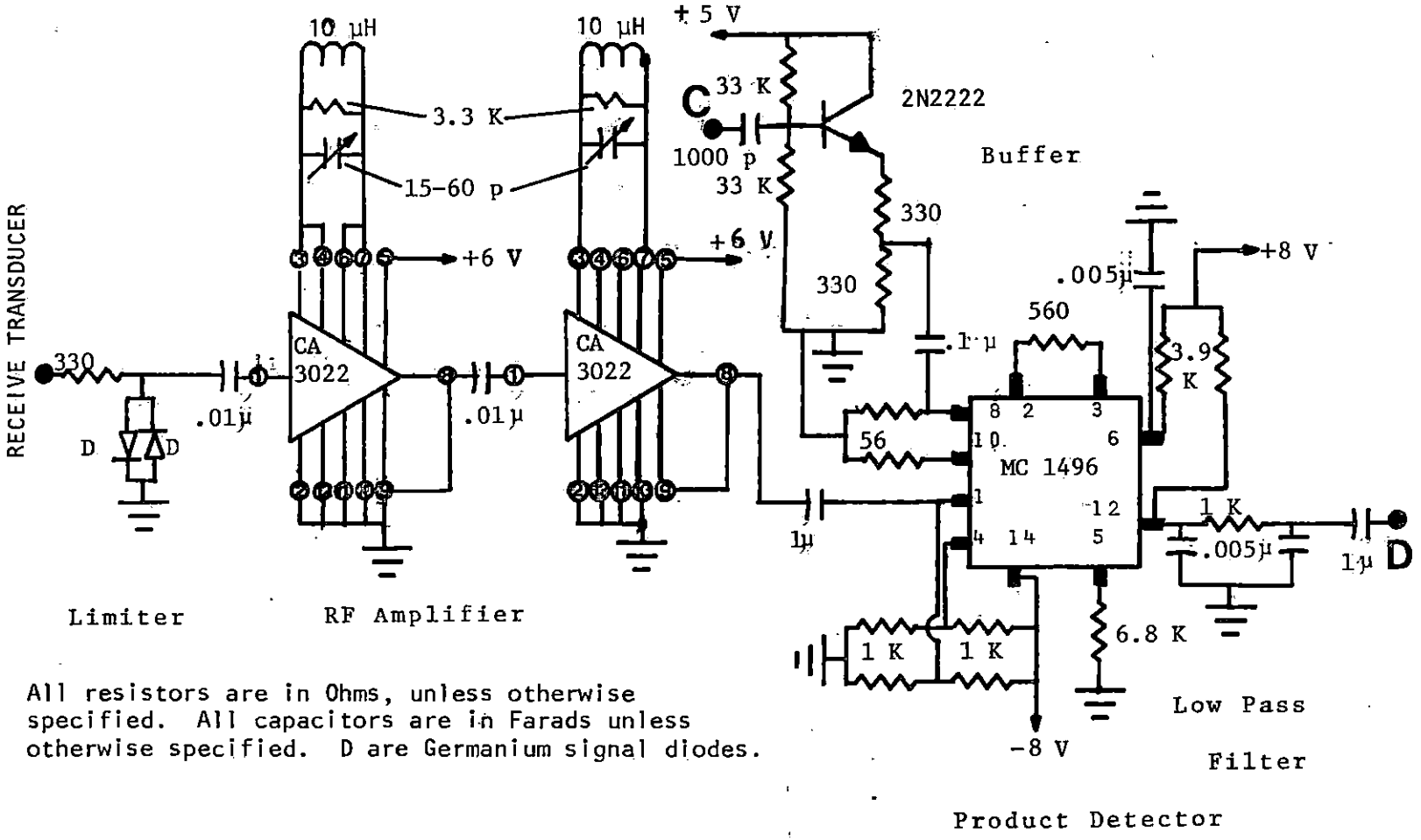

All resistors are in Ohms, unless otherwise specified. All capacitors are in Farads unless otherwise specified. D are Germanium signal diodes.

Figure 16. Schematic diagram of receiver and detector circuits

$$\text{Gain} = \frac{0.637\ R_l}{R_e + 2r_e} \tag{25}$$

where R_l = load resistance

R_e = emitter resistance between pin 2 and 3

r_e = transistor dynamic emiter resistance, at $25^{o}C$.

The output signal from the product detector is filtered through a two-pole low-pass passive filter with a frequency cutoff of 50,000 Hz. The output is connected to a sample/hold circuit. Prior to the sample/hold circuit is a buffer stage needed to drive the capacitive input of the sample/hold. The load resistance of the product detector is mainly the resistor connected to ground from the + input of the buffer stage. This ground resistor is equal to 27 KΩ. The gain of the product detector, considering a value of 25 Ω for the dynamic emitter resistance and a value of 560 Ω for R_e, is equal to 28 dB. The carrier from the local oscillator is passed through a buffer stage. The level of the carrier is about 300 mV RMS. Figure 16 gives the complete circuit diagram.

Range delay and sample circuits

The depth at which the Doppler signal is sensed within the blood vessel and tissue depends on the delay interval between the transmitted burst and the sample gate. For a velocity of sound in tissue of approximately 1500 m/sec, the range factor is 13.6 μsec per centimeter of depth.

A simple one-shot multivibrator is used to develop the range delay. The range delay potentiometer is coupled to a range dial calibrated in centimeters of depth. Figure 17 shows the delay circuit. With this calibration, it is a relatively simple matter to measure the sound path

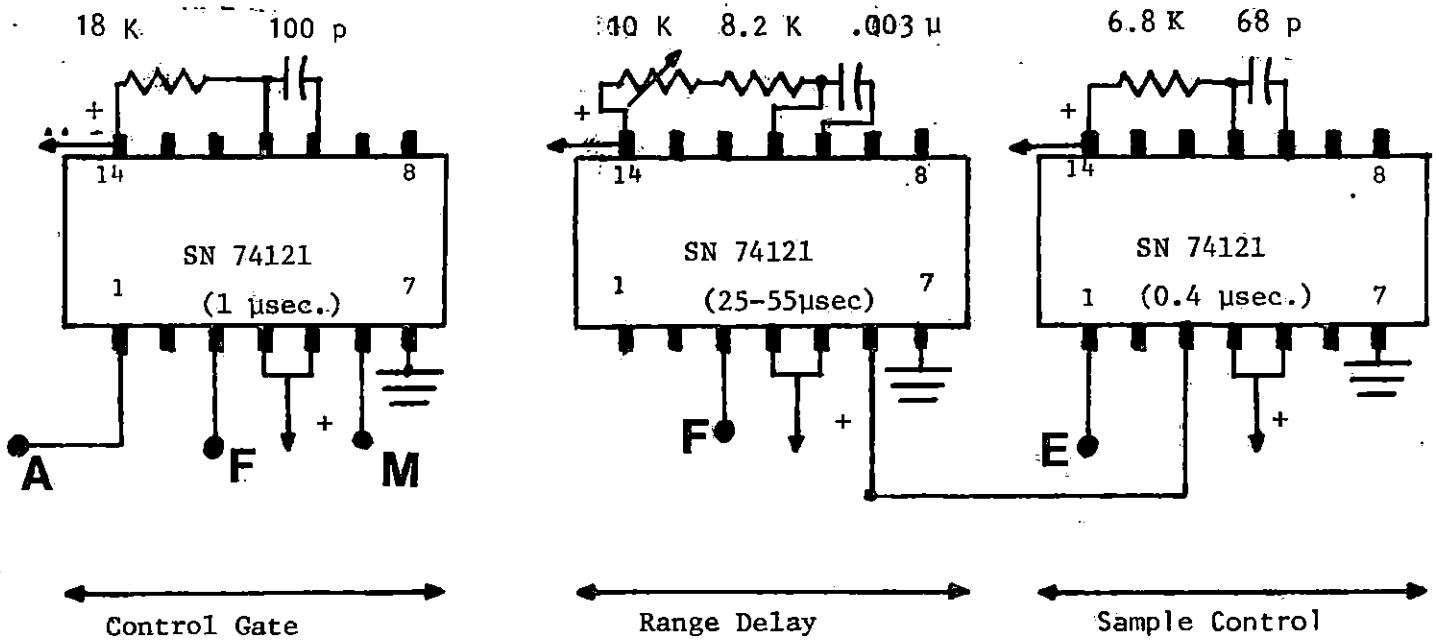

All terminals marked + are connected to +5 volts positive supply. All resistors are in Ohms unless otherwise specified. All capacitors are in Farads unless otherwise specified.

Figure 17. Schematic diagram of monostable multivibrator circuit

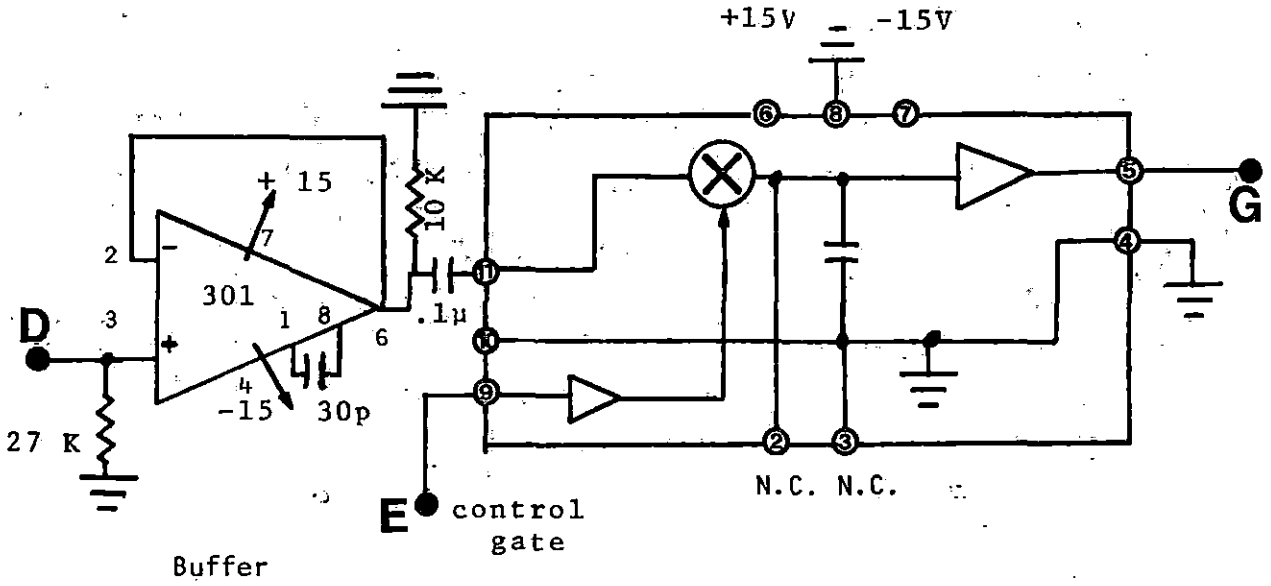

Sample and hold (Datel Corp. SHM-2)

All resistors are in Ohms unless otherwise specified. All capacitors are in Farads unless otherwise specified.

Figure 18. Schematic diagram of sample/hold and isolation amplifier circuits

length that intercepts a blood vessel by noting the depth at which they disappear. If the angle between the sound beam and the blood vessel is known, then the true vessel diameter can be determined. A sample gate is actuated by the range delay multivibrator. The duration of the pulse from the sample gate generator depends on the type of Doppler detection that is desired. Baker (22) suggests two methods of detection.

Method 1 This method is used when a velocity measurement with maximum sensitivity is required at a specific point in the blood vessel. This discrete measurement will be necessary when mapping the velocity profile within a blood vessel. Precise determination of the lumen diameter of a vessel will also necessitate the discrete sensing of velocity to determine the margins of blood flow at the vessel walls. This maximum-resolution, maximum-sensitivity operation is achieved by using a broad-band transducer, a short transmitted pulse duration of 0.5 μsec or less, and a boxcar-type sample and hold circuit following the product detector. The signal from the product detector, indicating a modulation in amplitude, is sampled by a gate that is turned on for only 0.1 μsec. This sample is stored in a capacitor. The capacitor voltage is held until the next transmitted burst and subsequent sample. Figure 18 illustrates the circuit diagram of the sample/hold and buffer circuits.

This detection scheme appears to have the maximun possible gain for conversion (of the pulse that is amplitude modulated) to a voltage representing the Doppler difference frequency between the transmitted and received ultrasonic wave.

The spatial resolution cell or sample volume in the blood vessel, in this method is dependent on the dimensions of the acoustical packet in the blood rather than the duration of the sample pulse. Tests indicate that the packet is approximately 1.5-2.5 mm in length (depth) and has a cross-section approximated by the sound beam diameter at the range (depth) of the sample. The packet length is determined by the duration of the burst applied to the transmitting transducer and the bandwidth of the transmitting and receiving elements. The detected Doppler shift frequency will correspond to the mean velocity averaged over the sample volume. As a result, the larger the vessel diameter compared with the dimensions of the sample volume, the more accurate will be the measurement of velocity profile and of diameter. Average velocity over the vessel cross-section can be measured by another method.

Method 2 Rather than scan across the vessel with a high resolution small sample volume in an attempt to measure the velocity profile, it is possible to sample the entire vessel diameter at one time and have a direct readout of the average velocity.

The output of the product detector is sampled in the same manner as in Method 1 except that the sample duration is set to extend across the vessel lumen diameter.

Since there is a velocity distribution across the vessel (profile), there will be a corresponding Doppler shift distribution developed when the entire lumen is sampled simultaneously. When the detected Doppler shift is coupled to a zero-crossing meter, the meter will indicate the mean frequency and, hence, the mean velocity.

Audio preamplifier and filters

A pair of active filters were used in the pulsed ultrasonic Doppler system. An active high pass filter with unity gain follows the sample and hold circuit. The cutoff frequency is about 50 Hz. This is a Butterworth filter with an attenuation slope of 40 dB/decade. The high-pass section comes first to remove the large amplitude, low-frequency spatial leakage components. These leakage components vary widely when the transducer is moved intentionally or from random motion.

Following the high-pass section, there is a low-pass filter used to remove the high-frequency PRF components from the detected Doppler signal. The selection of the roll-off frequency depends on the PRF and on the highest expected Doppler frequency. Usually, the highest PRF that avoids range ambiguities is used. This PRF rate is almost always above the highest Doppler shift frequency. Therefore, the filter should be set to roll off just above the upper Doppler limits rather than at one-half the PRF. This procedure tends to improve the detector Doppler signal-to-noise ratio. The cutoff frequency is set at 8000 Hz with an attenuation slope of 40 dB/decade and with unity gain. The latter is also a Butterworth filter.

The reason that the filters are placed before the audio preamplifier is because the signals coming out of the sample and hold contain low-amplitude Doppler components and relatively high-amplitude components from the transmitter pulse repetition rate. In addition to the Doppler frequency, there are signals due to spatial leakage changes that extend down to D.C. and are large in amplitude. They could easily block any high-gain amplifier that was connected directly to the sample circuit output.

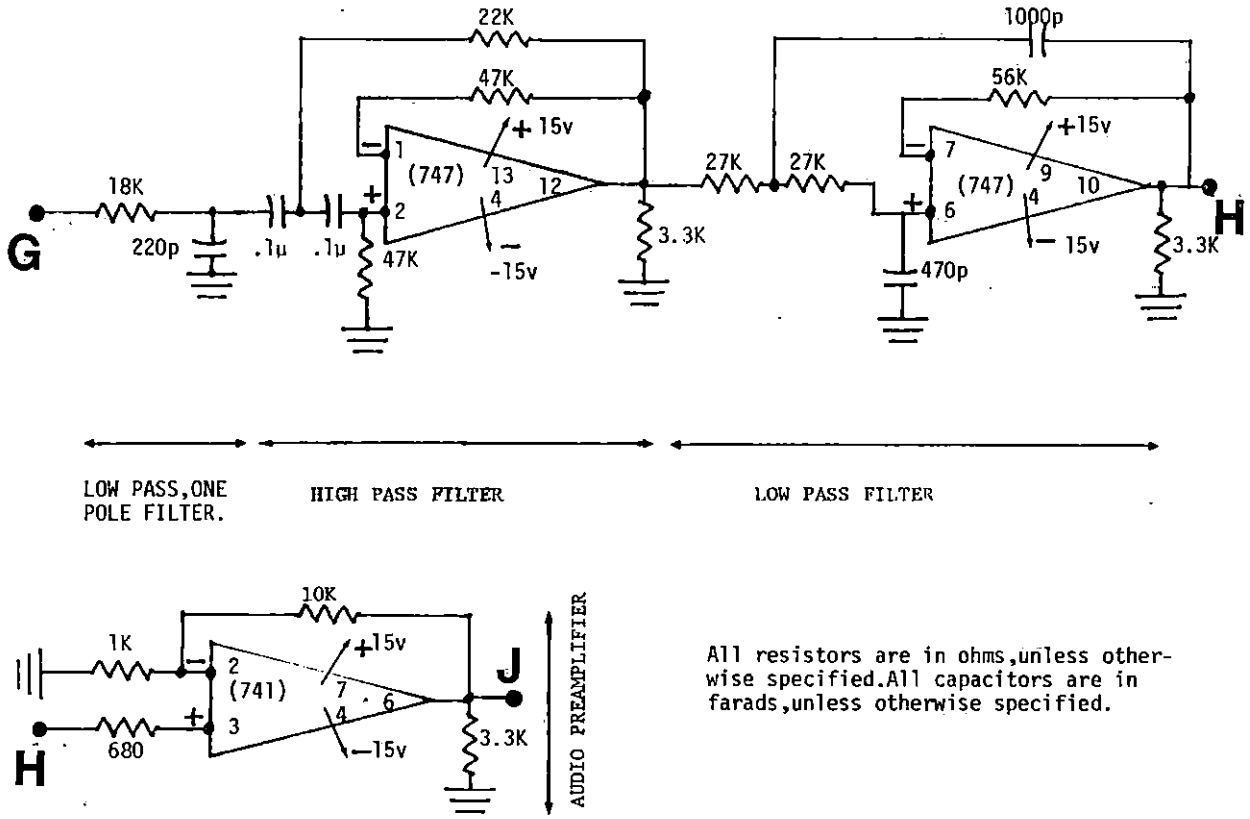

All resistors are in ohms,unless otherwise specified.All capacitors are in farads,unless otherwise specified.

Figure 19. Schematic diagram of the audio preamplifier and filters

An audio preamplifier with a band-pass exceeding the maximum filter bandwidth and a gain of 10 follows the filters. The Doppler signal is raised to 0.5 Volt level in order to be able to drive an external audio power amplifier and/or a frequency-to-voltage converter. Figure 19 shows the complete circuit diagram of audio preamplifier and filters.

Frequency-to-Voltage converter

In order to measure fluid velocity, a frequency meter is required. Nearly all commercial Doppler velocimeters use Zero Crossing Detectors (ZCD), since they are simple and inexpensive.

The ideal ZCD consists of a comparator that gives an output pulse every time the voltage of the electrical signal crosses the zero line going from negative to positive. The output from the detector is normally obtained by averaging the number of pulses over approximately 50 msec. The ZCD can give erroneous information by triggering from electrical noise. This results in a very high output level when it should be zero. This problem can be overcome by using an offset trigger level.

Since the ZCD output is the root mean square of the input frequency and not the mean, a change in flow profile will affect the output from the detector even though the mean velocity remains constant (22).

The frequency-to-voltage converter used in this research is an integrated circuit manufactured by Analog Devices Corp., type 451J. Figure 20 shows the circuit diagram that performs the frequency-to-voltage conversion. It is set to give an output of 1 Volt for each KHz of frequency. The device has a frequency response up to 11 KHz.

It features a variable threshold trigger input level from 0 to 0.7 Volts and hysteresis of 50 mV_{p-p}.

RMS-to-D.C. converter

The output signal from the frequency-to-voltage converter, shows the frequency spectra as a function of time when displayed in an oscilloscope. In many cases we are interested in the average frequency which corresponds to the average flow from the Doppler shifted frequency. This operation is performed accurately by an RMS-to-D.C. converter. The device used is an integrated circuit made by Analog Devices Corporation (type AD 540 J). Figure 20 shows the complete circuit diagram of the RMS-to-D.C. converter with a one pole "post" active filter at the output. The device features analog processing blocks inside the chip. One of the problems associated with signals that are random, as in the case of Doppler shifted signals, is obtaining a minimum ripple with a fast settling time. The former problem can be tackled simply by connecting a bigger ripple capacitor. On the other hand, for any step change the settling time might be too long. This problem can be compromised by using a capacitor value to achieve lower ripple rejection but faster settling time. A better approach is to add a one-pole filter at the output of RMS-to-D.C. converter. This approach will be a better solution to both problems. This latter approach was considered in the design of the system.

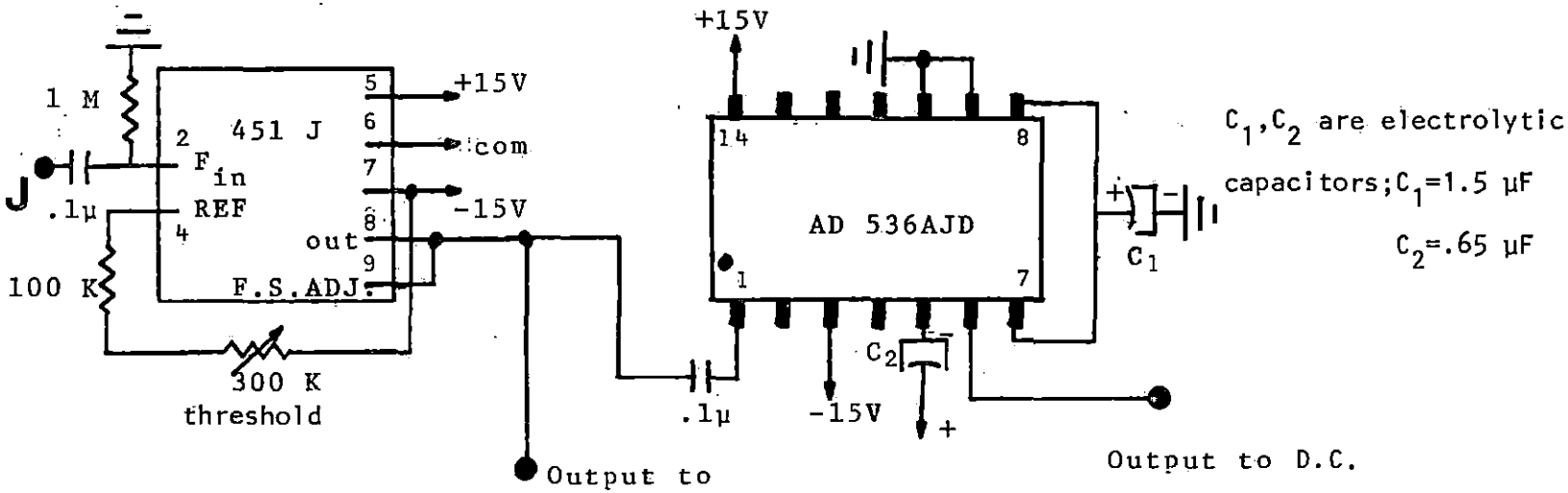

Frequency-to-voltage converter.

RMS-to-D.C. converter

All resistors are in Ohms unless otherwise specified.

All capacitors are in Farads unless otherwise specified.

Figure 20. Schematic diagram of the frequency-to-voltage converter and RMS-to-D.C. converter circuits.

EXPERIMENTAL METHODS

The experiments were conducted under two different flow conditions, peristaltic pump and constant head tank.

Condition 1: Generated Flow by Means of Peristaltic Pump

In this experimental arrangement, a peristaltic pump produced the flow necessary to test the accuracy of the device. The tube which carried the flow to the test bench was a normal plastic tube; its construction is not relevant.

In the test bench region, a thin-wall latex tube ($\frac{1}{4}$ inch diameter) was used in testing the performance of the instrument. The choice of material and thickness was made to avoid any probable attenuation by the wall of the tube. The test region of the tube was submersed in a water-filled styrofoam tank. This material minimizes reverberation within the tank produced by the walls. The tube was placed inside a groove on the floor of the tank; this prevented any movement of the tube and thereby avoided creation of any unwanted signals. Immersing the tube in water provided an acoustical coupling between the transducer and the fluid. Also a set travelling time from the transmitter to the receiver is accomplished.

Two transducers, one for receiving and one for transmitting, were used. The chosen transmitting frequency was coincident with the natural frequency of the crystal transducers.

A Sarns model #3500 portable peristaltic pump having with variable speed and reverse flow possibilities was used. The flow generated by this pump was pulsatile.

Each transducer was attached to a micromanipulator device. One of the micromanipulators could measure angles. Zero degrees coincided with the transducer being perpendicular to the floor of the tank. The transmitter and the receiver were both placed at an angle of 80 degrees from the horizontal.

The output from the frequency-to-voltage converter was recorded on a Hewlett-Packard model #3960 instrumentation tape recorder. The speed used during recording was 15 inches per second (ips). Only one channel was used in this experiment. During playback the speed was 3/4 ips. The tape output was connected to a Beckman model #R611 pen-writing recorder. This time expansion was necessary in order to slow down the frequency of the events, since the Beckman recorder does not have sufficient response to clearly record the Doppler signal that occurred in the experiment. The playback signal was also processed through the RMS-to-D.C. converter and recorded. The sensitivity of the paper recorder instrument was set at 50 mV/mm. The paper speed was 10 mm/sec. Recordings were made for three different values of volume flow. Only the average and not the instantaneous volume flow for each value was measured. This was done by connecting an analog voltmeter at the output of the RMS-to-D.C. converter. The analog voltmeter had a sensitivity of 20,000 ohms per volt. A 10 μF electrolytic capacitor was connected in parallel with the input to the voltmeter in order to reduce ripple. For each value of volume flow, three readings were taken from the voltmeter. The mean value of the three reading was used as a measured value. Following each measurement of volume flow, three control readings of volume flow were made using a calibrated beaker and stop watch. The flow values were averaged.

In order to test the accuracy of the range capabilities of the pulsed ultrasonic device, the diameter of the tube at the test region was measured. The audio preamplifier was connected to an audio amplifier and speaker. An oscilloscope was used to display the control signal that was applied to the boxcar sample and hold circuit. The diameter of the tube was determined by noting when the flow signal appeared as the range gate was scanned across the lumen and then again when it disappeared. Taking the difference in range at each of these points gave the diameter. The true diameter can be computed if the angle of the transducer with the vessel is known. Figure 21 shows the schematic diagram of this experimental arrangement under the control condition.

Condition 2: Generated Flow From a Constant Head Tank

This experimental arrangement ensured a parabolic flow profile by keeping the differential pressure head constant, and hence allowed accurate estimation of the mean flow velocity.

The experimental procedure for condition 2 was identical to that for condition 1, except for the difference in flow profile.

In order to warrant the type of flow generated under the two different conditions (turbulent flow with condition 1 and laminar flow with condition 2), the Reynolds number (R_n) was calculated for each case. A turbulent flow was assumed for $R_n > 3000$ and laminar flow otherwise.

Whole milk was the fluid used to scatter the ultrasonic wave in both conditions. Figure 22 shows the schematic diagram of the experimental arrangement under this second control condition.

Figure 21. Schematic diagram of experimental arrangement for condition 1

Figure 22. Schematic diagram of experimental arrangement for condition 2

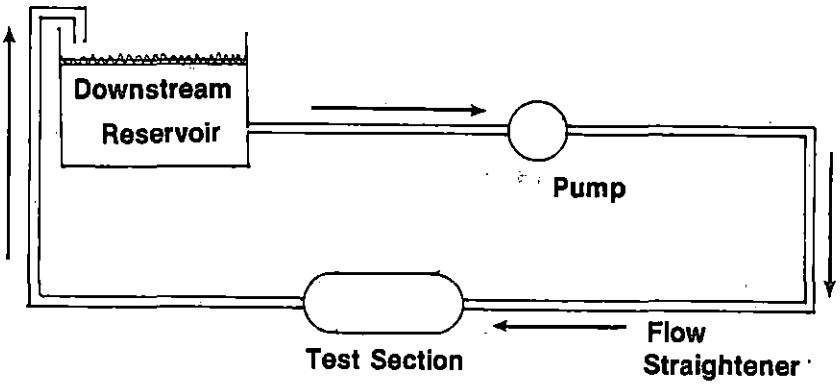
Downstream
Reservoir
Pump
Test Section
Flow
Straightener

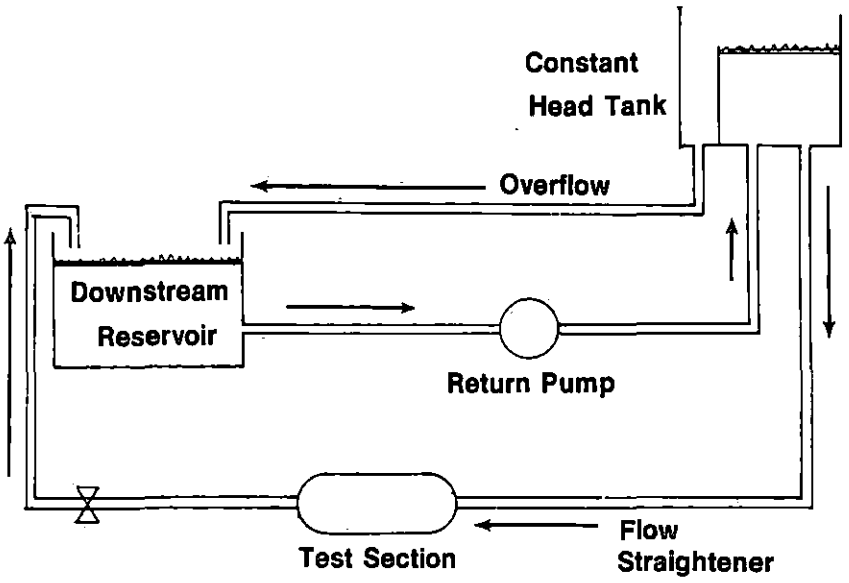
Constant
Head Tank
Overflow
Downstream
Reservoir
Return Pump
Test Section
Flow
Straightener

RESULTS

The results of the experiments under control condition 1 were very satisfactory. Table I lists the values of measured and control values. The values of volume flow measured with the Doppler shift ultrasonic flowmeter versus control values of volume flow are plotted in Figure 23. The straight line was plotted from the experimental data points, using linear regression techniques. The percentage error[1] for each set of comparison values is also shown. These values of errors are within the range published by different authors (13).

Figure 24 shows the frequency spectra from Doppler shifted signal versus time. Figure 25 shows the average values of the frequency spectra.

The range capability of the device was only tested in the measurement of the lumen diameter. The time difference between the starting and end of the rush from the fluid flow was 5 μsec. If considering a travelling time/cm by the ultrasonic wave of 6.5, the distance travelled by the wave during that period is $5/6.5 \simeq 0.77$ cm.

Taking into consideration the angle between the probe and vessel equals 80°, we have

$$D_t = \cos 10^{\circ} \times 0.77 = 0.76 \text{ cm} \qquad (26)$$

where D_t = true diameter of the lumen.

The real inside diameter was equal to 0.63 cm. As can be seen from the last expression, the difference between measured and real diameter is within the tolerance quoted in the literature (13).

---

[1] Percent absolute error is calculated as

$$\frac{\text{Volume-Flow (Doppler)} - \text{Volume-Flow (Control)}}{\text{Volume-Flow (Control)}} \times 100.$$

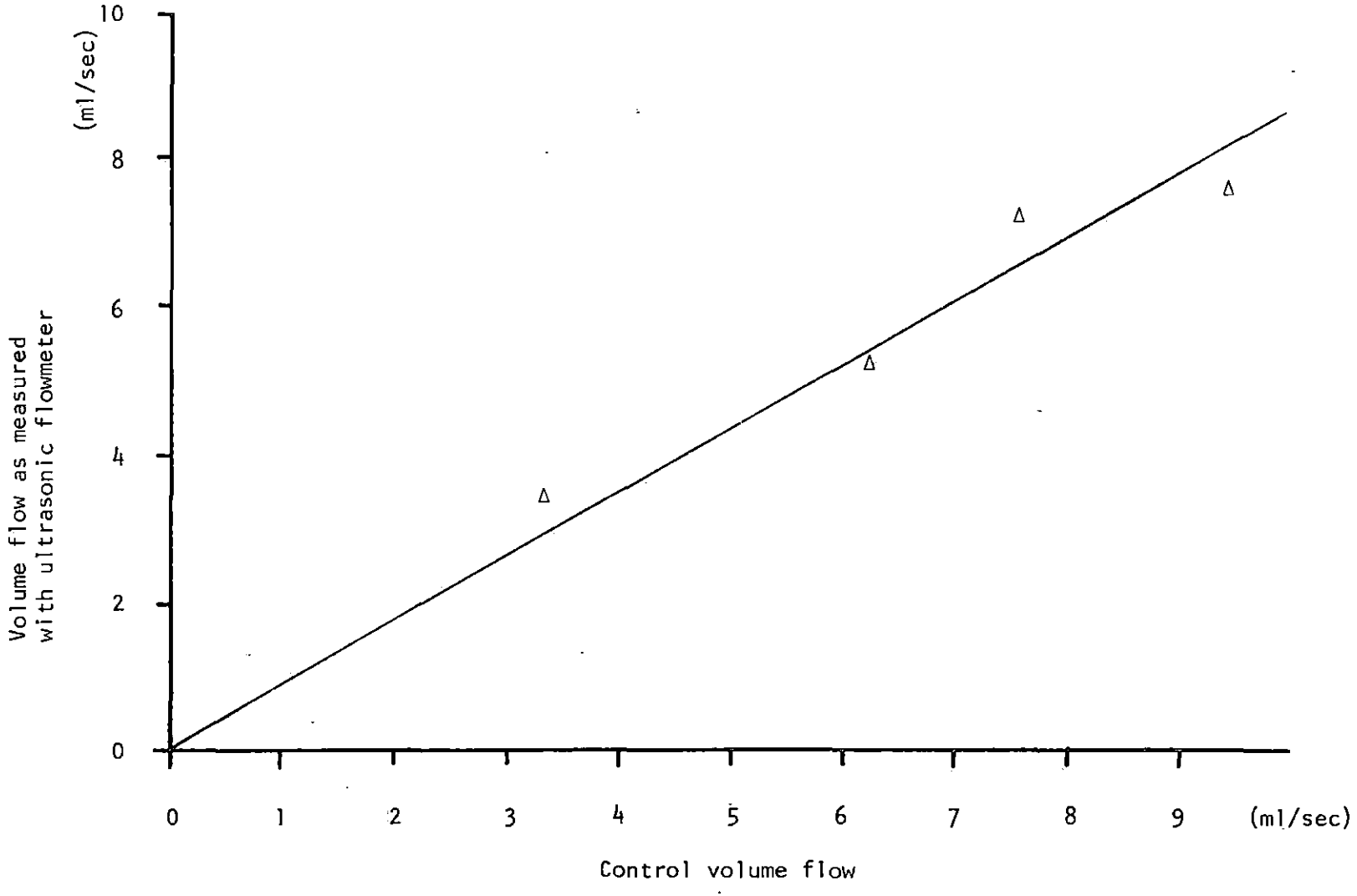

Figure 23. Graph of measured volume flow using ultrasonic Doppler shift instrument versus control values of volume flow

Table 1. Comparative values between measured volume flow and control volume flow (control condition 1)

Average Doppler shifted frequency $\overline{\Delta f}$ (Hz)	Average computed volume flow $\overline{Q}_D$ (ml/s)	Average control volume flow $\overline{Q}_C$ (ml/s)	Absolute error %E
189	3.52	3.32	+ 6
281	5.21	6.21	- 16
383	7.1	7.5	- 5.3
406	7.53	9.35	- 19

Results of the experiment under control condition 2 were also very satisfactory. Table 2 shows the result. See also Figure 26.

Table 2. Comparative value between measured volume flow and control volume flow (control condition 2)

Average Doppler shifted frequency $\overline{\Delta f}$[a] (Hz)	Average computed volume flow $\overline{Q}_D$ (ml/s)	Average control volume flow $\overline{Q}_C$ (ml/s)	Absolute error %E
115	2.13	2.18	- 2.2
142	2.62	2.43	+ 7.8
149	2.76	2.61	+ 5.7

[a]The average frequency is taken from a sample Doppler region located at the center of the vessel. This value actually is the maximum velocity of fluid flow. The average is calculated as: $\overline{\Delta f} = f_{D.max}\ 0.57$.

Figure 24. Frequency-time plot of Doppler difference frequency taken with ultrasonic pulsed range-gated flowmeter for relatively: (a) low; (b) medium; (c) high; volume flow

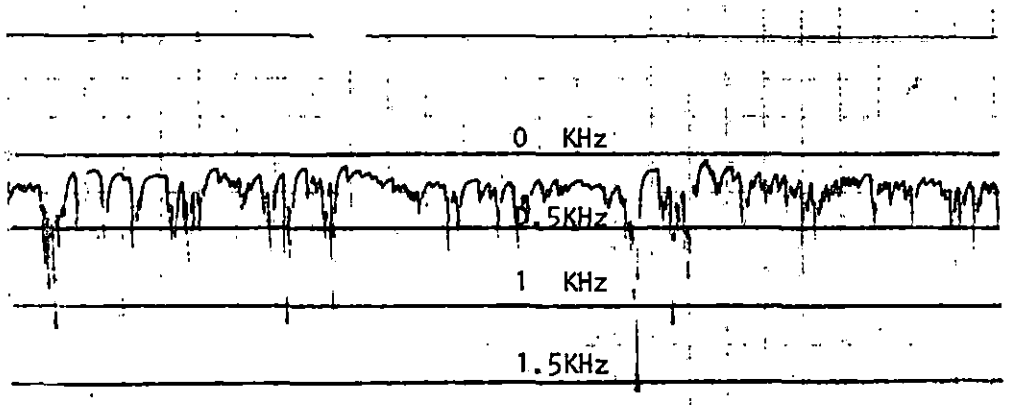
0 KHz
0.5KHz
1 KHz
1.5KHz

(a)

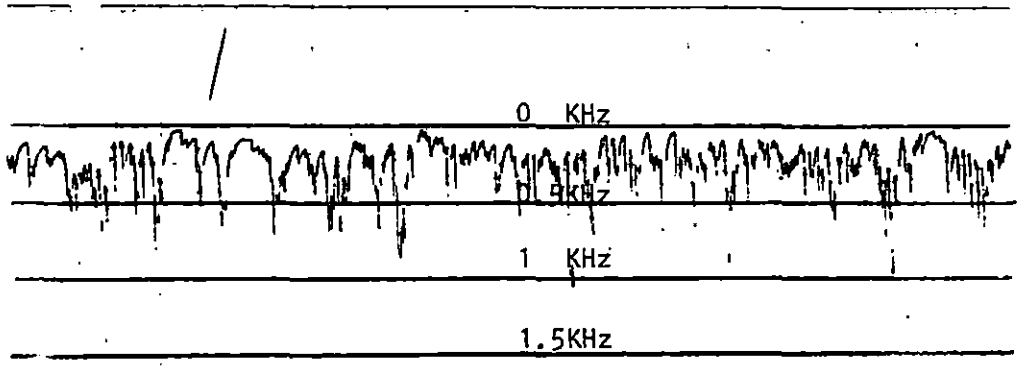
0 KHz
0.5KHz
1 KHz
1.5KHz

(b)

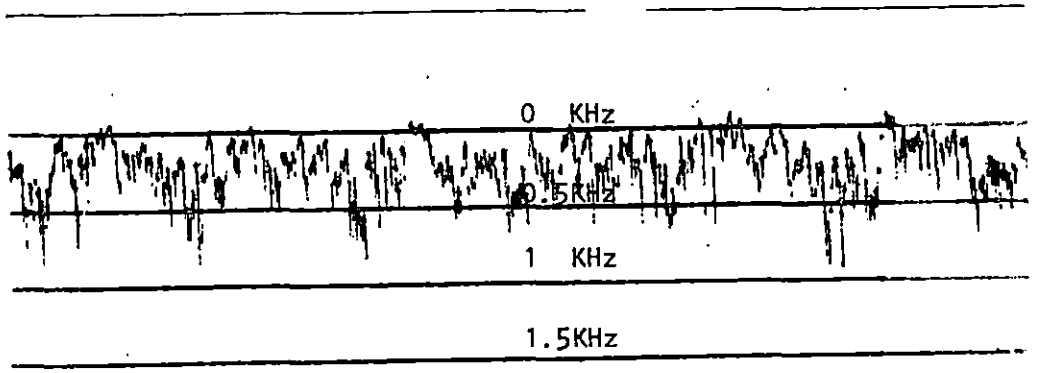
0 KHz
0.5KHz
1 KHz
1.5KHz

(c)

Figure 25. RMS values of frequency Doppler shifted signal versus time as taken from previous spectra for relatively, (a) low, (b) medium, (c) high volume flow

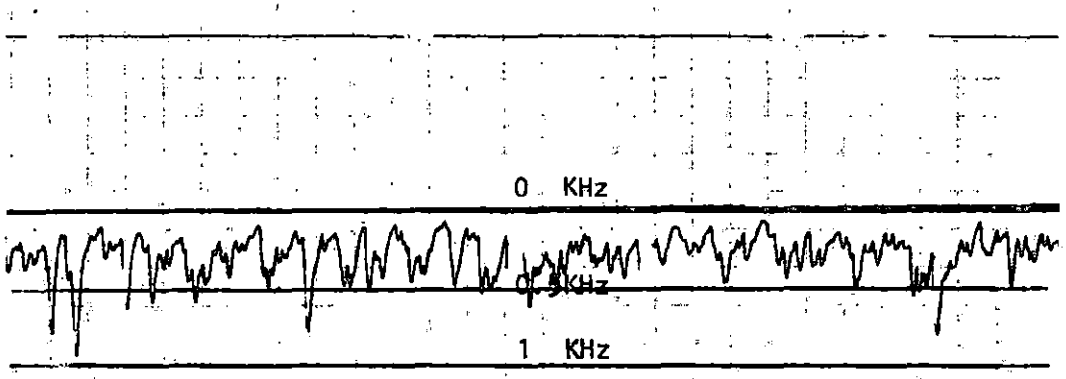

(a)

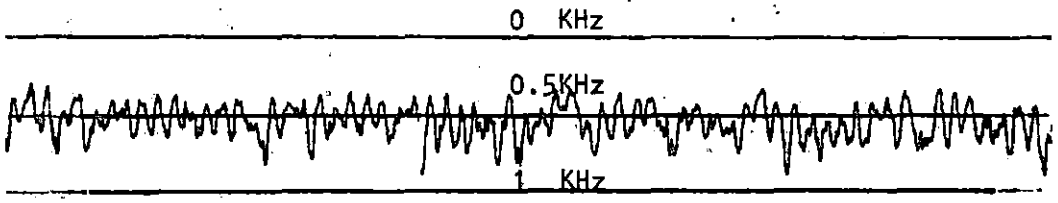

(b)

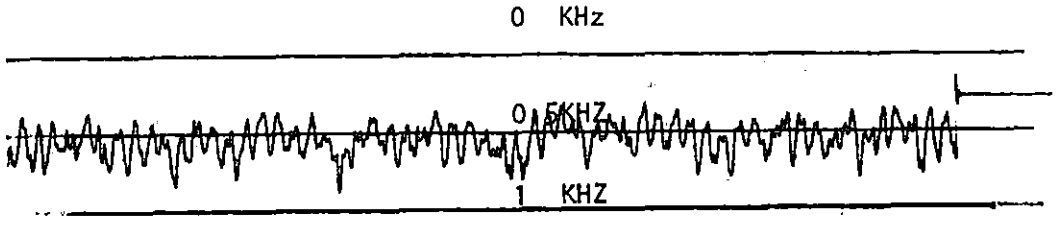

(c)

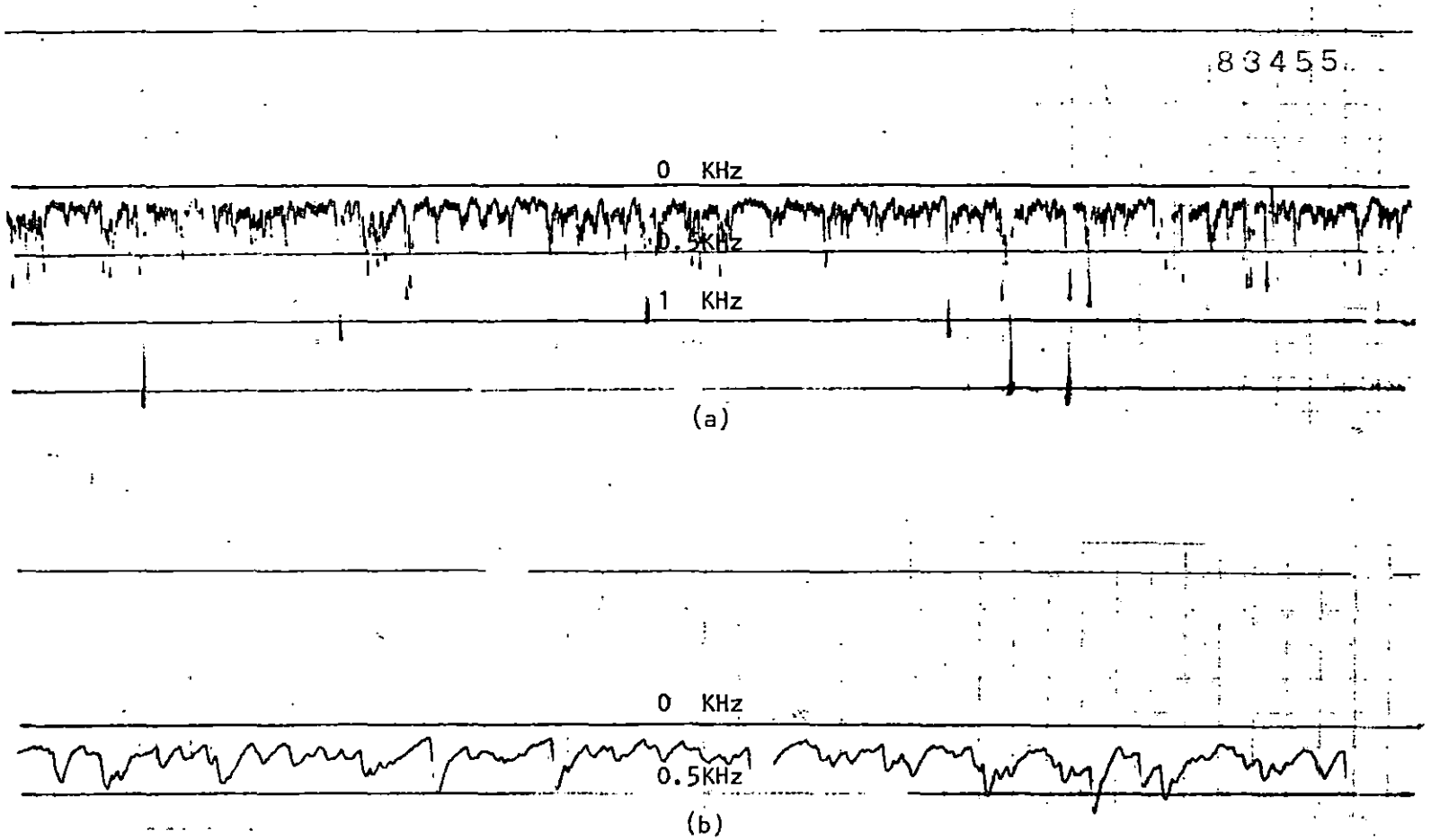

Figure 26. Frequency-time plot of Doppler difference frequency taken with ultrasonic pulsed range-gated flowmeter, from a constant head tank. (a) Relatively medium volume-flow. (b) RMS value from the previous graph

DISCUSSION

The pulsed Doppler instrument designed was only tested "in vitro" for computation of average volume flow. Within the limits of its spatial resolution, the pulse Doppler technique can be an effective tool for investigating dynamic velocity profile in models on animals and on man. Baker (22) mentions a technique first used by Peronneau et al. (18). Their profiles were made by scanning across the vessel or tube at a slow rate and then reconstructing the profile over many cycles.

This method is adequate if the pulsatile flow is absolutely periodic. Unfortunately, physiologic flows do not have this well-behaved property (22). A pulse Doppler instrument of the type being described here can be arranged to operate with suitable additions so as to measure the flow velocity at many sites similtaneously across the lumen of a vessel. This can be accomplished by adding more sampling channels, all in parallel. This effectively forms a comb type gate instead of the single gate described previously.

Each channel output will give the velocity at the range set for that channel; with the use of a sequential gate generator, the first burst can bet set to start at any range and produce a sample at range increments from 0.5 mm spacing upward. A profile can be constructed in real time by sampling the channels at high speed, in sequence, and then displaying velocity as a function of range.

One of the features that would have been convenient to have was the flow direction capability. In the project described in this paper a VCO originally was used to achieve this feature. The reason that

direction capability could not be accomplished was because VCO design was implemented with NAND gates. Three gates were used for the VCO section and one gate was used for gating the signal coming from the oscillator section. A monostable gives the control signal to achieve the total width of the pulse train. It was not possible to obtain any reading or hear any sound from the instrument. It is believed that the reasons lie in the shape of the output waveform (square wave) from the oscillator and the poor gating of the logic gate.

Due to time constraints, the building and testing of a VCO with sinusoidal output and a satisfactory gate (good ON/OFF ratio) was not possible. In order to minimize the leakage from the oscillator section, good gating is a must.

The receiver tested in this project, although having performed reasonably well, should have had a higher gain. Operation with a single transducer would be advisable. This would necessitate a quick recovery time from the transmitter transients in the receiver. In order to attenuate echoes from targets situated close to the transducer a combination of MOS-FET dual gate devices followed by bipolar transistors stages would be the right choice.

It remains to be evaluated whether a receiver with deliberate limiting for the purpose of quieting would reintroduce sidebands for all conditions of received signals. Hard limiting is advisable to use since it produces a significant amount of quieting from the removal of the amplitude components from the Doppler shifted echoes. From the listening test common to investigators using Doppler techniques,

it was quite apparent when quieting occurred with the resulting suppression of white noise. Under some conditions of received signal, the quieting can be as much as 40 dB improvement in the signal-to-noise ratio (22).

It would also be convenient to have some discussion of the influence of flow profile in the analysis of the frequency spectra from Doppler shifted signals by means of zero crossing detector. For steady flow in a rigid tube, theory shows that the profile is parabolic. Pulsatile pressure in the body causes the flow profile to be nonparabolic, and in the great arteries it can become flat with all the blood moving at the same velocity. Very asymmetric and peaky profiles can be expected close to bifurcations and just distal to stenoses. For each of the various flow profiles, the number of cells travelling in each velocity range can be calculated assuming that the cells are evenly distributed across the vessel. Thus, the expected Doppler shift spectrum can be derived provided that each cell scatters the same amount of ultrasonic energy. From this spectrum, the mean frequency and the theoretical zero crossing frequency can be calculated and compared (25). With a flat profile the mean frequency of the zero crossing detector (f_{zc}) is equal to the mean frequency ($\overline{f}$), with a parabolic profile f_{zc} increases to 1.16 $\overline{f}$ and with the more peaky profiles to and near stenoses f_{zc} can increase further (25).

The pulsed Doppler flowmeter described in this research has a wideband power amplifier. This is convenient if different frequencies with different transducers want to be experimented. Simply by changing the LC

values of the resonant circuit of the receiver section, the center frequency received can be changed.

It can be suggested that a microprocessor can be instructed to solve equation (23) to compute the volume flow. It can be extended further to instruct the microprocessor to analyze the frequency spectra by FFT, making the device small in size and capable to analyze the signal in real time.

BIBLIOGRAPHY

1. Satomura, S. 1959. A study of the flow patterns in peripheral arteries by ultrasonics. Journal of the Acoustical Society of Japan 15:151-158.

2. Wells, P. N. T. 1969. Physical Principles of Ultrasonics Diagnosis. Academic Press, London.

3. Wells, P. N. T. 1969. A range-gated ultrasonic Doppler system. Medical and Biol. Engng. 7:641-652.

4. Yoshida, T., M. Mori, Y. Nimura, G. Hikita, S. Takagishi, K. Nakanishi, and S. Satomura. 1961. Analysis of heart motion with ultrasonic Doppler method and its clinical application. Am. Heart J. 61: 61-75.

5. Yoshitoshi, Y., K. Machii, H. Sekiguchi, Y. Nishina, S. Ohta, Y. Hanaoka, Y. Koshashi, and H. Kuno. 1966. Doppler measurement of mitral valve and ventricle wall velocities. Ultrasonics 4:27-28.

6. Lube, V. M., Y. U. D. Safonov, and L. I. Yakimenkov. 1967. Ultrasonic detection of the motions of cardiac valves and muscle. Soviet Phys. Acoust. 13:59-65.

7. Johnson, W. L., H. F. Stegall, J. N. Lein, and R. F. Rushmer. 1965. Detection of fetal life in early pregnancy with an ultrasonic Doppler flowmeter. Obstet. Gynec., N. Y. 26:305-307.

8. Rushmer, R. F., D. W. Baker, N. L. Johnson, and D. E. Strandness. 1967. Clinical applications of a transcutaneous ultrasonic flow detector. J. Am. Med. Assn. 199:325-328.

9. Fielder, F. D. and P. Pocock. 1968. Foetal blood flow detector. Ultrasonics 6:240-241.

10. Hunt, K. M. 1969. Placental localization using the Doptone fetal pulse recorder. J. Obstet. Gynaec. Br. Commonw. 76:144-147.

11. Strandness, D.E., R. D. Schultz, D. S. Sumner, and R. F. Rushmer. 1967. Ultrasonic flow detection. A useful technic in the evaluation of peripheral vascular disease. Am. J. Surg. 113:311-320.

12. Emslie, A. G. and R. A. McConnell. 1947. Radar System Engineering. Ed. L. N. Ridenour. McGraw-Hill, New York.

13. Baker, W. D., F. W. Forster, and R. E. Daigle. 1978. Doppler principles and techniques. Pages 161-287 in F. J. Fry, ed. Ultrasound: Its Applications in Medicine and Biology. Elsevier, New York.

14. Thompson, F. J. 1978. Broadband pulsed Doppler ultrasonic system for the non-invasive measurement of blood velocity in large vessel. Med. and Biol. Eng. and Comp. 16:135-146.

15. McLeod, F. D. 1974. Multichannel pulsed Doppler techniques. Pages 85-107 in R. S. Reneman, ed. Cardiovascular Applications of Ultrasound. North Holland Publishing Company, Amsterdam.

16. Reid, J. M. and D. N. Baker. 1973. Principles of Doppler ultrasound. Pages 411-422 in G. Baum, ed. Fundamentals of Medical Ultrasonography. J. P. Putnam and Sons, New York.

17. Gill, R. W. 1975. An implantable pulse Doppler ultrasonic blood flow meter using custom integrated circuits. Ph.D. Thesis. Stanford University. 288 pp. Dissertation Abstracts International 36:2389B-2390B.

18. Peronneau, P., H. Hinglais, M. Pellet, and F. Leger. 1970. Vélocimetre sanguin par effect Doppler à l'emission ultrasonore pulsée. L'onde Electrique 59:369-386.

19. Roevros, J. G. 1974. Analogue processing of C.W. Doppler flow meter signals to determine average frequency shift momentaneously without the use of wave analyzer. Pages 43-54 in R. S. Reneman, ed. Cardiovascular Applications of Ultrasound. North Holland Publishing Company, Amsterdam.

20. Brody, W. R. 1974. Theoretical analysis of the C.W. Doppler ultrasonic flow meter. IEEE Trans. Biomed. Eng. 21(3):183-192.

21. Rihaczek, A. N. 1969. Principles of High-Resolution Radar. McGraw-Hill Book Company, New York.

22. Baker, D. N. 1970. Pulsed ultrasonic Doppler blood-flow sensing. Transactions on Sonics and Ultrasonics 17(3):170-184.

23. Morris, R. L., M. B. Histand, and C. W. Miller. 1973. The resolution of the ultrasonic pulsed Doppler for blood velocity measurements. J. Biomech. 6:701-710.

24. Forster, F. K., J. I. Garbini, and J. E. Jorgensen. 1976. Hemodynamic turbulence measurements using ultrasonics techniques. Pages 253-256 in Proc., 4th New Eng. Bioeng. Conf. S. Sana, ed. Pergamon Press, New York.

25. Lunt, M. J. 1975. Accuracy and limitations of the ultrasonics Doppler blood velocimeter and zero-crossing detector. Ultrasound in Med. and Biol. 2:1-10.

26. Baker, D. W., D. E. Strandness, and S. L. Johnson. 1976. Pulsed Doppler techniques: Some examples from the University of Washington. Ultrasound in Med. and Biol. 2:251-262.

27. Hansen, P. L., G. Cross, and H. Strandness. 1974. Beam angle independent Doppler velocity measurement in superficial vessels. In J. P. Woodcock, ed. Clinical Blood Flow Measurement. Sector Publishing, London.

28. McCarthy, K. and J. P. Woodcock. 1974. The ultrasonic Doppler shift flowmeter - a new development. Biomed. Eng. 9(8):336-341.

29. Franklin, D., S. A. Borders, and W. S. Kemper. 1977. Frequency modulated, pulsed, range gated sonar method for soft tissue imaging and blood flow measurement. Pages 1831-1833 (Vol. 3B) in D. White and R. E. Brown, eds. Ultrasound in Medicine. Plenum Press, New York.

ACKNOWLEDGMENTS

I wish to express my appreciation to the many people who have assisted and advised in the project, in particular the staff members of the Biomedical Engineering Program. Especially I wish to thank Dr. David L. Carlson, my major advisor, for his guidance, help, and his patient attitude in advising in the different phases of the design process. I am also grateful to Dr. Curran S. Swift and Dr. Paul R. Bond for serving on my graduate committee and also giving correct advice throughout this project.

A special note to my parents who have provided support and encouragement throughout my formal education.